IN VIVO IMAGING OF THE HEMATOPOIETIC STEM CELL ENGRAFTMENT PROCESS IN THE MOUSE TIBIA BONE

By

SEUNGBUM KIM

A DISSERTATION PRESENTED TO THE GRADUATE SCHOOL
OF THE UNIVERSITY OF FLORIDA IN PARTIAL FULFILLMENT
OF THE REQUIREMENTS FOR THE DEGREE OF
DOCTOR OF PHILOSOPHY

UNIVERSITY OF FLORIDA

2011

To my mother in heaven

ACKNOWLEDGMENTS

I had many people around me who supported and encouraged my work while pursuing my doctorate degree. First of all, I would like to thank my mentor Dr. Edward Scott for his guidance and support in both science and life. It was his mentorship and vision that lead me to study science with great joy. Secondly, I would like to thank my committee members Drs. Maria Grant, Chris Cogle and Dietmar Siemann for their support and advice. The passion and effort to science that I felt from them I will remember. In addition, I must thank all Scott lab members especially Dr. Liya Pi, Li Lin Gary Brown, Dustin Hart, Drs. Koji Hosaka, Greg Marshall and Mark Krebs for their help and advices. I will cherish memories I had with my fellow graduate students, Jeff Harris, Nic Bengtsson, Huiming Xia, Anitha Shenoy and David Lopez. I would also like to thank the staffs of the core facilities at UF, Neal Benson, Marda Jorgensen, Doug Smith and Mike Rule for their support and expertise. Finally, I would like to thank my family members. Without the unconditional love and support from my wife Jiyoung Choi, my precious daughters Jiwu and Jisu, my parents Sung-Yong Kim and Il-Mi Kim and my sister Jung-Eun Kim, nothing I have accomplished to date would have been possible.

TABLE OF CONTENTS

page

LIST OF FIGURES

LIST OF ABBREVIATIONS

BM	Bone marrow
CFU-S	Colony forming unit - spleen
c-Kit	Stem cell growth factor receptor CD117
D	Day after cell transplantation
FACS	Fluorescence Activated Cell Sorting
h	Hour after cell transplantation
HSC	Hematopoietic stem cells
HSPC	Hematopoietic stem and progenitor cells
IHC	Immunohistochemistry
Lin	Lineage markers
LT-HSC	Long-term HSC
MSC	Messenchymal stem cell
Sca-1	Stem cell antigen 1
SLAM	Signaling of lymphocytic activation molecules
SLAM-SKL	SLAM expressing Sca-1 positive, c-Kit positive, Lin negative cells
SKL	Sca-1 positive, c-Kit positive, Lin negative cells
Tp	Transplantation

Abstract of Dissertation Presented to the Graduate School
of the University of Florida in Partial Fulfillment of the
Requirements for the Degree of Doctor of Philosophy

IN VIVO IMAGING OF THE HEMATOPOIETIC STEM CELL ENGRAFTMENT PROCESS IN THE MOUSE TIBIA BONE

By

Seungbum Kim

December 2011

Chair: Edward William Scott
Major: Medical Sciences – Molecular Cell Biology

A fundamental question in stem cell biology is where stem cells reside and how stem cell niches control stem cell activity in vivo. Although the hematopoietic stem cell (HSC) is well characterized, our current knowledge of where and how transplanted HSPCs become engrafted is very limited. HSC transplantation is now routinely done in clinics to correct a variety of bone marrow deficiencies. Considering its extensive use, understanding the HSPC engraftment process has now become critical if we are to improve the treatment strategies. A key to understanding HSC engraftment is to be able to observe the process in vivo. I aimed to visualize fluorescent HSC in the mouse tibia bone directly by grinding one side of the tibia until the bone was sufficiently thin for direct observation. By making a “window” into the tibia bone, I was able to observe the very early engraftment process of a single HSC lodging and proliferating at the bone marrow niche. The Sca-1+, c-Kit+, Lin- (SKL) cells preferred to prosper mainly on the osteoblastic niche. In contrast, further purified SKL, CD48-, CD150+ population (SLAM-SKL) was mostly observed in the perivascular niche. When mice were co-transplanted with DsRed+ SKL and GFP+ SLAM-SKL populations, SKL cells were 25 times more than SLAM-SKL cells in the bone marrow at Day 7. However, contribution of each

population to the blood circulation at the same time was not consistent. It was extramedullary hematopoiesis observed from the spleen that produced extra amount of blood from SLAM-SKL cells, which suggests that the SLAM-SKL cells engrafted in the perivascular niche in both BM and spleen and can support hematopoiesis much quicker than SKL cells. This study shows a novel technique to understand and highlight the dynamic process of the stem cell engraftment in complex microenvironment of the bone marrow.

CHAPTER 1
BACKGROUND AND SIGNIFICANCE

Hematopoietic Stem Cell Niche in the Bone Marrow

The concept of bone marrow transplantation was established in early 1960 (1). However, it was impossible to define cells with stem cell activity such as self-renewal or proliferation at that time. But scientist already knew the existence of more primitive cells in the bone marrow and the population was defined by the ability to initiate colony formation in spleen. Spleen colony forming unit (CFU-S) was a very similar concept to today's HSC as it has the ability to differentiate any blood cell lineage and undergo unlimited proliferation (2-4). These studies pointed out that there are higher concentration of the CFU-S in the bone surface that in the center of the BM. The findings that bone marrow cell populations are shown to conform to a well-defined spatial organization corresponding to the chronologic relationships between marrow cells led to the idea of the HSC niche by Schofield that the stem cell is maintained in close association with a microenvironment which supports self-renewal and prevent differentiation and maturation (5-9). When this stem cell-niche association is perturbed, the stem cell is thought to be committed to a specific lineage of the blood cells and loses its stem cell property (Figure 1-1).

Spatial Distribution of Transplanted HSC in the BM

In the past, in-depth analysis of tracing the transplanted BM cells was restricted by the technologies available to detect donor cells in the recipient. To allow cell tracking, techniques including analysis of cell surface markers expressed on donor cells such as the Ly5.1/5.2, β-galactosidase, Southern blot analysis to detect Y chromosome-specific DNA sequences in male donor cells within female recipients and fluorescent in situ

hybridization (FISH) were utilized (10-14). Another way of monitoring the donor cells was to dye the membrane of the donor cells with hydrophobic and lipophilic cyanine dyes such as PKH-26, which had shown to provide information on the fate of transplanted HSCs in the BM and spleen (15). However, this approach is greatly limited by the number of cell divisions of the donor cells as the dye fluorescence was diluted by half with each cell division (16). As a result, the use of fluorescent dyes to track transplanted HSCs may be limited to short-term analysis. Using another fluorescent dye carboxyfluorescein diacetate succinimidyl ester (CFSE), Nilsson et al. labeled different subpopulations of BM cells for transplantation in nonablated recipients and analyzed the lodgment of engrafted cells (17). This study clearly demonstrated that there is spatial distribution of HSCs and HPCs in the bone marrow, according to their respective level of lineage commitment. Specifically, although the majority of primitive cells that lacked markers of hematopoietic lineage commitment and cells that were committed to a particular hematopoietic lineage (Lin+) localized in the central marrow region immediately after transplantation, Lin- cells selectively redistributed away from the central marrow region and predominantly localized in the endosteal region, whereas Lin+ cells selectively redistributed away from the endosteal region and predominantly localized in the central marrow region (17, 18).

Factors and Chemokines Involved in the HSC Niche

In the adult mammal, hematopoiesis is restricted to the extravascular compartment where HSCs are in contact or close proximity with a heterogeneous population of stromal cells in the bone marrow. Cellular interactions between HSCs and stromal cells involve tightly co-ordinated participation of various cell surface molecules such as integrins, selectins, sialomucins and chemokines such as osteopontin, CXCL-12 and

SCF (Figure 1-2, (19)). I will introduce P-selectin, osteopontin and CXCL-12, the three critical factors that were used in data presented here.

P-selectin

A variety of cell adhesion molecules have been described that mediate contact between the hematopoietic cells and the microvascular endothelium, including selectins, a family of glycoproteins that include L-selectin, E-selectin and P-selectin (20, 21). Several studies have suggested that members of the selectin family of glycoprotein adhesion molecules may be candidate mediators of this angiogenic process (Figure 1-3 and Ref. 20). In particular, P-selectin, a constitutively expressed endothelial determinant that is critical to leukocyte-endothelial adhesion is upregulated in response to variety of factors, including hypoxia and inflammation (22). However, characterization of the recently described P-selectin positive cells is only in its initial stages, and whether P-selectin positive endothelial cells in the bone marrow sinusoid plays a critical role in HSC engraftment is not clear.

Osteopontin

Osteopontin (OPN) is an acid-rich, multi-domain, phosphorelated glycoprotein. Within the bone marrow, the most prominent source of OPN is osteoblasts and therefore, OPN has a highly restricted expression to the endosteal surface (23-25). Preosteoblast, osteocytes but not mesenchymal cells or fibroblasts can also synthesize OPN(26, 27). OPN is bound by multiple integrins such as α4β1, αvβ3, α5β1, αvβ5. Many of these OPN binding integrins recognize the RGD-binding sequence of OPN. OPN can also bind to ECM such as fibronectin and collagen, or minerals such as Calcium (26). OPN has been well studied in bone regulation and recently, OPN is appreciated in HSC and tumor biology (28). OPN is the key molecule in attraction and

regulation of HSCs in the endosteal niche. The most compelling evidence of OPN regulating HSCs is from studies using OPN-/- mice. Several studies demonstrated that OPN is a negative regulator of HSC proliferation (24, 25). The OPN null microenvironment in the BM was sufficient to increase the number of stem cells associated with increased stromal Jagged1 (24). The other study showed that the HSCs isolated from OPN -/- mice fed with BrdU exhibited extensive incorporation of BrdU which again suggest that OPN plays a direct role in the maintenance of HSC by inhibiting entry into the cell cycle (24).

CXCL12

During embryogenesis and adult life, HSC migrate to various organ sites and retention of HSC in a specific anatomic location is also mediated by chemokines. CXCL 12 or Stromal-derived factor-1 (SDF-1) and its receptor, CXCR-4, are the most important regulatory pathway during ontogeny and adult life (29). HSC migration from fetal liver to the localization in the BM microenvironment was disrupted in transgenic mice deficient in CXCR-4 or SDF-1 (30, 31). These findings were further confirmed by a transplantation experiment of CXCR-4-deficient fetal liver cells into wild-type recipients, which revealed increase of circulating myeloid and lymphoid precursors in the blood, suggesting poor retention of stem cells in the BM (32). Investigations into CXCR-4 expression and function in CD34+ cells obtained from distinct tissue sources have demonstrated that despite lower levels of CXCR-4, responsiveness of the cells to SDF-1 was proportionally the highest in cells derived from the BM (33). This suggested that preserved chemokine receptor signaling was highly associated with BM rather than blood localization, further confirming the role of SDF-1 and CXCR-4 in HSC homing and lodgment (18).

Microenvironment to Form HSC Niches

At normal physiological state, hematopoiesis occurs in the bone marrow. The microenvironment of the bone marrow is rather dynamic than inert state, bone structure undergoing a constant process of remodeling via a tight coupling between bone formation from osteoblasts derived from mesenchymal stem cells, and bone resorption by osteoclasts, which are hematopoietic cell origin (34). A number of different cell types of the BM play crucial roles for HSC maintenance, quiescence and differentiation (Figures 1-4 and 1-5), (35, 36). In this chapter, three most important cell types that comprise the HSC niche will be introduced.

The Osteoblastic Niche

Osteoblasts are located along endosteum, the inside lining of the bone facing bone marrow. The most imporatnt functions of osteoblasts in bone remodeling are the secretion of unmineralized bone matrix proteins that constitute bone structure (37). Several studies had shown that the osteoblastic niche plays a critical role as part of the regulating microenvironment or niche for HSCs (34, 38). Zhang et al. reported that conditional knockout of BMP receptor 1A triggered a significant increase of the N-cadherin positive osteoblast and was correlated to the increase of the HSC in the bone marrow (38). Additionally, SNOs express membrane bound stem cell factor (mSCF, KitL, steel factor), which has been shown to be crucial in both niche retention and in maintaining HSC quiescence (39, 40). In another report, mice with constitutively activated parathyroid hormone receptor in the bone had significantly increased JSC in conjunction with increased trabecular osteoblasts that expressed Jagged1(34). Parathyroid hormone had also been suggested to directly modulate the osteoblastic niche and affect HSC engraftment process *in vivo* (34, 41). The interaction between

osteoblast and HSC is further confirmed by an experiment with conditional osteoblast deletion in mice (42). When osteoblasts numbers were reduced, the number of HSCs within the BM also decreased, resulting in extra-medullary hematopoiesis in spleen. Additionally, calcium sensing receptors (CaR) have also been implicated in the retention of HSCs in the endosteal niche (43). It is important that these *in vivo* works were initiated due to several in vitro experiments that osteoblast can support HSC ex vivo in cell culture system (44-46).

The Perivascular Niche

Endothelial cells line all sinusoid vessels in the BM and they are therefore the initial site of entrance of all blood cells into the bone marrow from the circulation and also the exit point where more mature blood cells leave the bone marrow into the bloodstream (47). The possibility of a perivascular zone serving as a regulatory niche for stem cells is originated from two important studies. One was from *In vivo* imaging study of primitive hematopoietic cells in animals over time and HSC seemed to be localized to specific subsections of the marrow microvasculature where cells persisted or increased in number over a 70 day interval (48). The experiment demonstrated that the perivascular microenvironment could act as a potential niche. However, it should be noted that the hematopoietic populations studied were not highly enriched for HSC in this study and it is very difficult to distinguish the border between the osteoblastic and perivascular niche in the microenvironment of the calvarium bone. Another important finding was from the discovery of SLAM antigens that enabled marking of HSCs by histologic assessment to understand where the HSCs resided in the marrow microenvironment (49). The studies indicated that the HSC purified by SLAM markers (CD150+, CD48-, CD41-, Lin-, 0.0067% of the BM cells) are the better stem cell

population and that only 14% of this HSC population were at the endosteal surface, while the majority of HSCs were in the perivascular region (62% adjacent to sinusoid, 95% near sinusoid). More recently, Rafii and colleagues have shown that the endothelial cells were essential for HSC self-renewal and engraftment of HSC depended on VEGFR2 mediated regeneration of endothelial cells (50, 51). These data suggest that the perivascular regions serve as a niche, but several caveats must be kept in mind. The most important is that the HSC that used with SLAM markers is not same compared to other cells to study osteoblastic niche. It is possible that the population has entirely different characteristics and cell dynamics compared to the traditional SKL cells. Another important point is that HSCs traffic into and out of the vasculature, so it remains possible that the cells accumulate around vessels just because it is an impedance point in their trafficking (Figure 1-6), (52). As such, this site would not meet the criteria for a niche which is a site where self-renewal should occur (53).

The Stromal Niche

Researchers hypothesized that there may be other cell types than endothelial cells that support HSC maintenance in the bone marrow (21). The hypothesis was confirmed by a recent publication by Mendez-Ferrer et al. (54). This group identified that one of the stromal cell type, the nestin positive messenchymal stem cell (MSC) which was closely associated with HSC. Majority of the nestin positive MSC were perivascular, but few of them were also present in the immediate vicinity of the endosteum. Interestingly, the nestin+ MSC were tightly associated with adrenergic nerve fibers of the sympathetic nervous system (SNS) that regulate HSC mobilization. It has been known that SNS were responsible for the circadian oscillations in circulating HSC

numbers (55, 56). Strikingly, these MSCs express higher levels of HSC maintenance factor transcripts, including SDF-1, SCF and angiopoietin-1 compared with any other stromal cell type including osteoblast (54). Most interestingly, nestin expressing MSCs show several similarities to recently identified mesenchymal progenitors by Nagasawa and colleagues (57, 58). Because of their high CXCL12 expression and their long cellular processes, these cells were named CXCL12-abundant reticular (CAR) cells. The majority of putative HSCs are found in close proximity to CAR cells by immunohistochemistry, and like nestin+ MSCs, CAR cells were predominantly found in the more central areas of the marrow, with some also located close to vessels near the endosteum. It needs to be determined whether the origin of the CAR cells and Nestin positive MSC is the same in the bone marrow.

In Vivo Imaging of the HSC Niche

To date, many significant discoveries have been made in regards to cell function, post-transplant localizations and pathology by the use of histological analysis of the transplanted cells and the development of transgenic mice. However, there are several caveats for these approaches. The use of the transgenic mice clearly demonstrates that there is a relationship between HSC and a certain niche cell population. However, it mostly explains the correlation of cell numbers among the populations and does not actually prove that the niche cell actually can regulate the HSC population. In addition, the HSC engraftment is a very dynamic process. Studies depended on the analysis of the engrafted cells in the bone histology in different time points (13, 14, 17, 19, 23). However, sections of the bone are not enough to show the true HSC distribution pattern in the live animal, because it is extremely hard to determine on histology whether the cells are actually tethering, migrating or lodging at the time of the sample collection. In

addition, most of the studies used SKL population and it is thought that only one in 25 SKL cells has the true stem cell potentials (59). Therefore, great emphasis has recently been put on being able to monitor cells engrafting on the bone marrow microenvironment *in vivo*. While histological analysis of tissues can only provide snapshots of a certain time point, *in vivo* imaging techniques have the potential to provide unique advantages in tracking cell migration, engraftment and fate analysis at multiple time points in the same study subject (60). One approach to imaging HSCs in the bone morrow was by mechanically removing part of the bone such as the mouse femur, and replacing it with a transparent glass cover slip to enable intravital viewing of the exposed marrow (61). Another approach, first demonstrated by Mazo, von Andrian and coworkers (20), took advantage of the relatively thin bone of the mouse skull, which allows optical imaging through the intact bone into the marrow cavities without the need for bone thinning. More recently, real-time live imaging has been utilized to track the migration of transplanted HSCs to the BM in irradiated and nonirradiated recipients (62, 63). These studies demonstrated that the transplanted cells can be tracked using the in vivo imaging techniques. However, ex vivo imaging does not exactly describe the engraftment event in vivo (63). Calvarium window is a less invasive method which does not disturb the subtle microstructures of the bone marrow (62, 64). However, the BM of the calvarium is smaller in volume and mixed with bone tissue which makes it hard to distinguish the exact location of the engraftment. Therefore, in vivo imaging of the long bone with a clear border between the bone and the BM, such as tibia and femur, is required to further understand the exact location of the HSC niche (64).

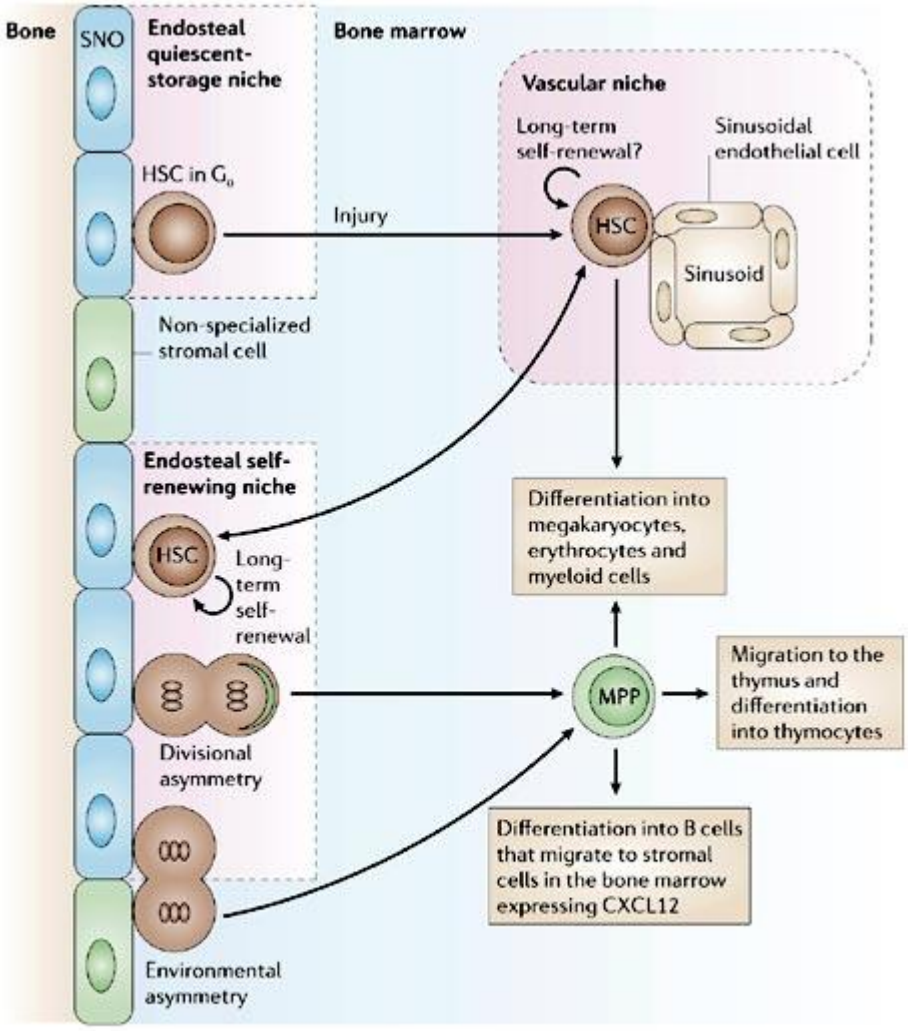

Figure 1-1. HSC asymemetric division and differentiation model in the HSC niche.

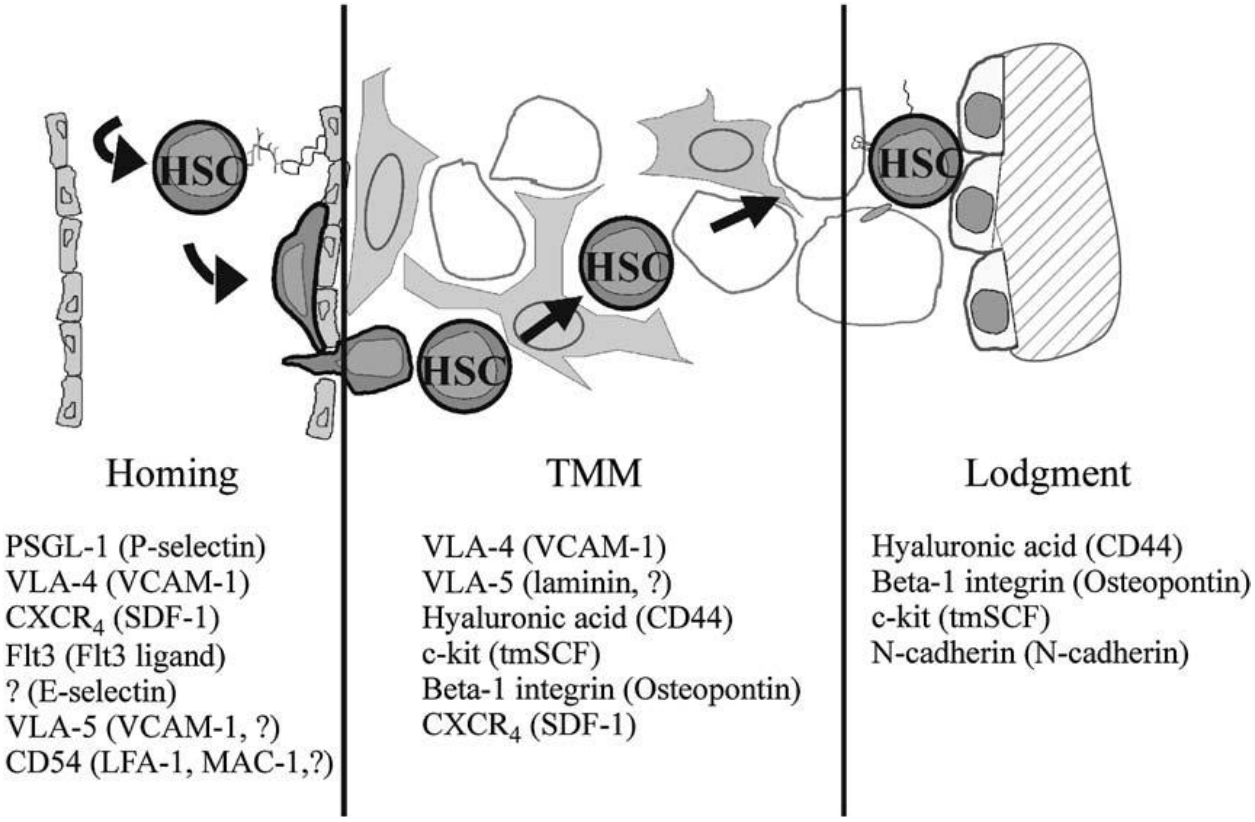

Figure 1-2. Cell surface ligand (receptor) interactions mediating the three phases of hemopoietic stem cell engraftment.

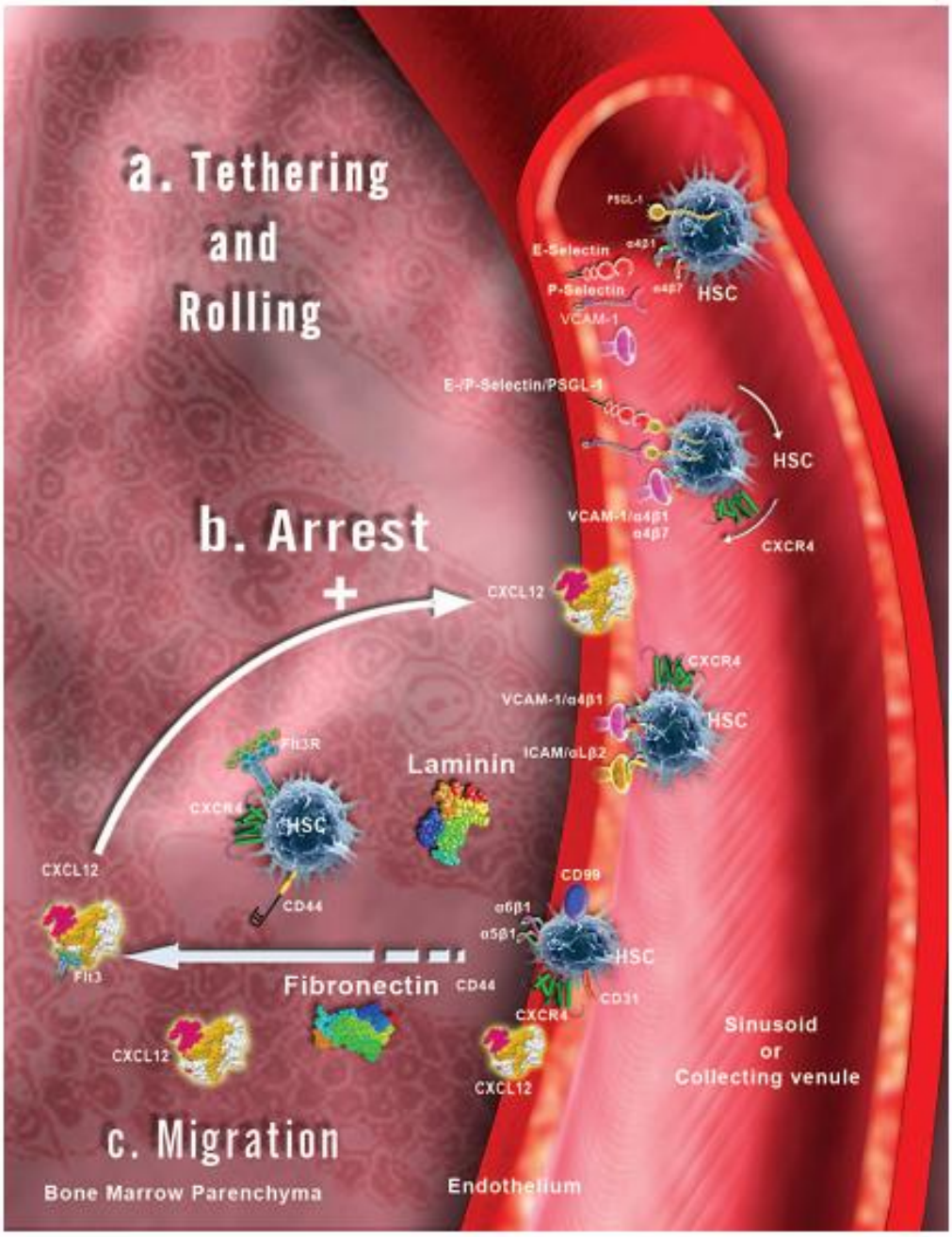

Figure 1-3. A model of HSC engraftment process in the very first stage and its molecular basis.

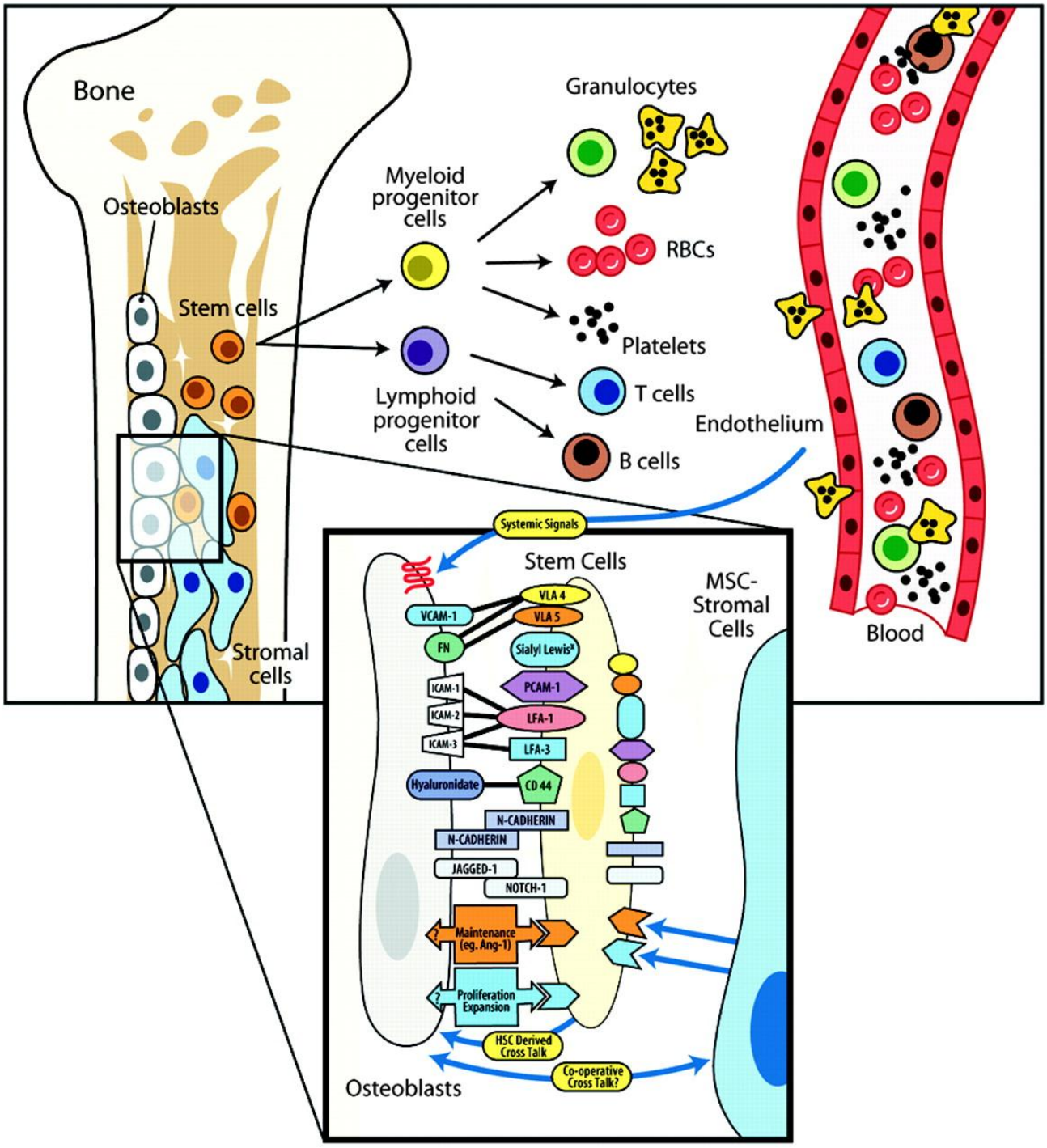

Figure 1-4. Hematopoietic stem cell in its niche. Various properties and cell surface markers have been proposed to explain the cell-cell interaction.

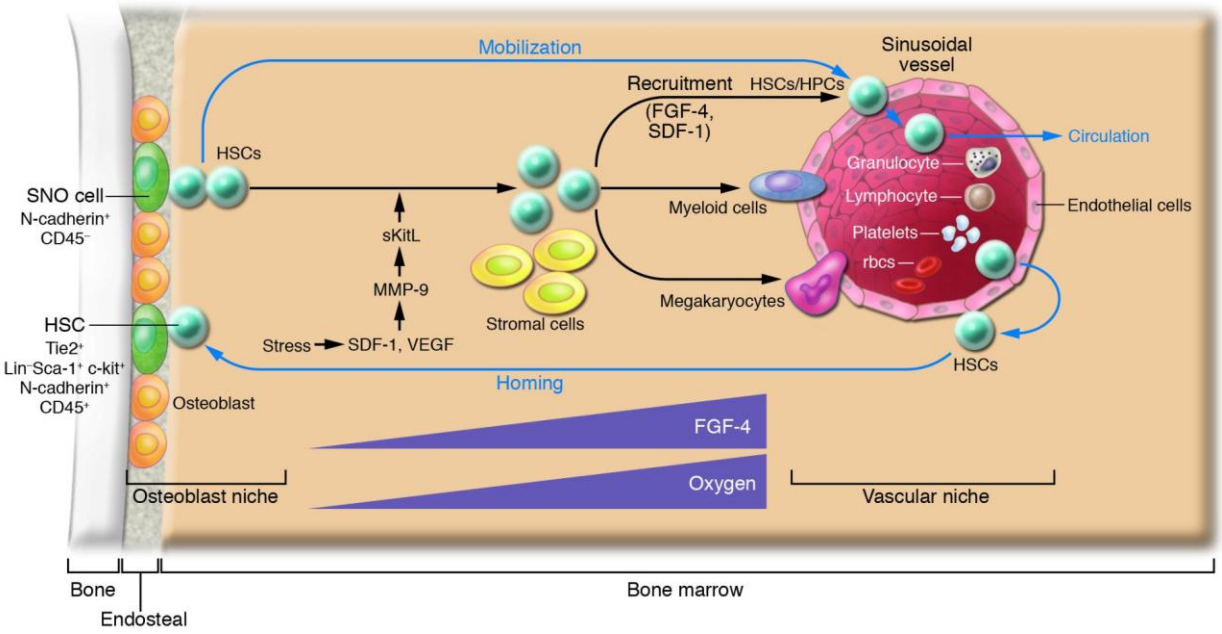

Figure 1-5. Homing and mobilization of HSC in the endosteal niche.

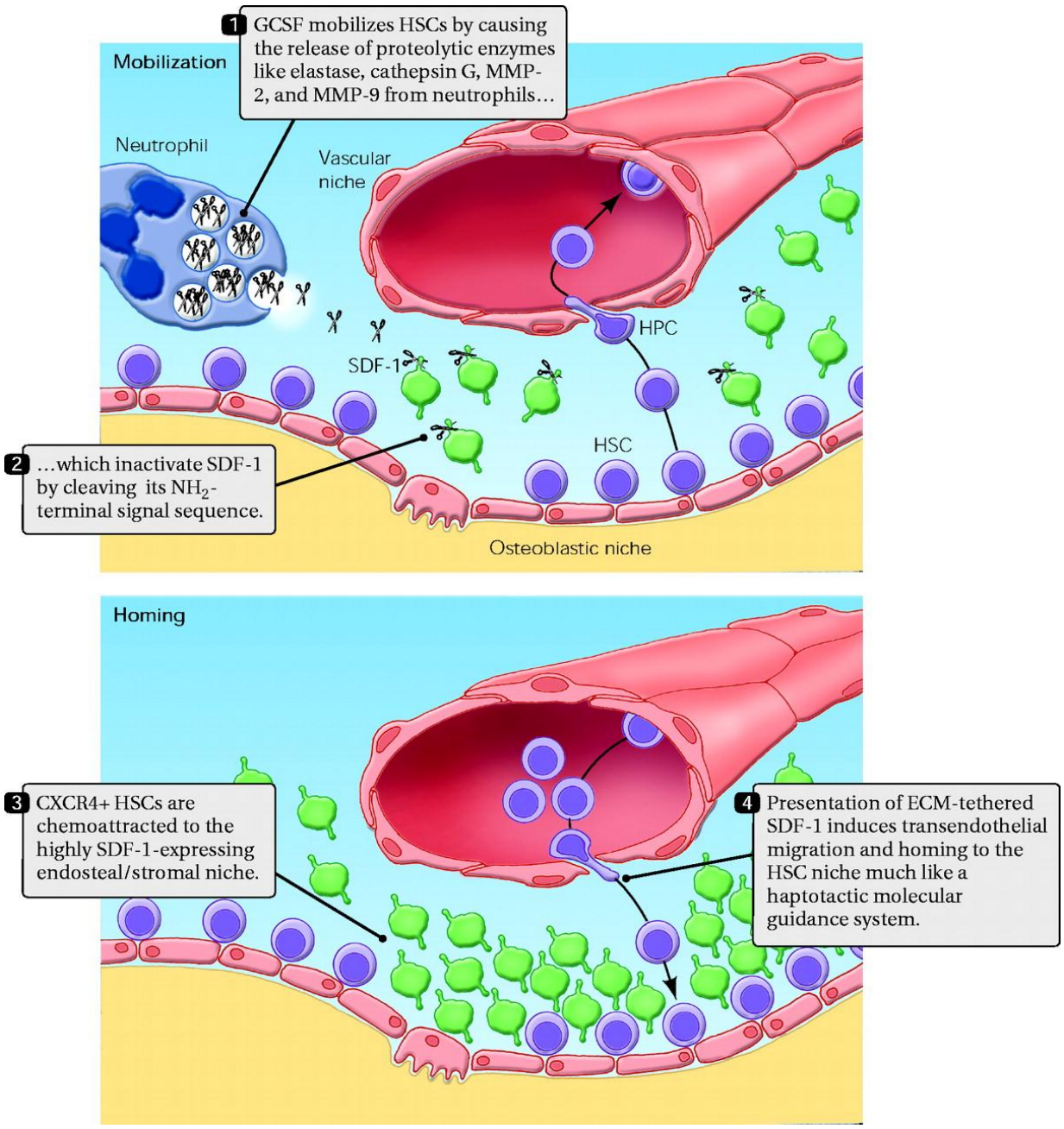

Figure 1-6. A model of HSC mobilization and homing processes.

CHAPTER 2
MATERIALS AND METHODS

The optimized materials and methods described in this chapter have been developed and adapted over a number of years from multiple previous reports and own observations.

Animals

C57BL6 mice were purchased from Charles River Laboratories (Wilmington, MA). C57BL/6-Tg(UBC-GFP)30Scha/J, Tg(CAG-DsRed*MST)1Nagy/J, 129S2-*Selp*^{tm1Hyn}/J (P-selectin knockout), B6.129S6(Cg)-*Spp1*^{tm1Blh}/J (Osteopontin knockout), NOD.Cg-*Prkdc*^{scid} *Il2rg*^{tm1Wjl}/SzJ (NOG) and Tg(TIE2GFP)287Sato/J mice were obtained from Jackson Laboratory (Bar Harbor, ME) and bred at the McKnight Brain Institute animal facility. All experimental procedures performed on animals were in accordance with the University of Florida's institutional review board and Animal Care and Use Committee.

Hematopoietic Stem Cell Purification

Bone marrow cells from UBC-GFP and DsRed mice for transplantation were age-matched. Bone marrow cells were flushed from tibiae and femurs of both legs into PBS supplemented with 1% FBS, 2mM EDTA, 25mM HEPES (FACS buffer). Cells were centrifuged at 1200 rpm for 5 minute at 4℃, passed through 20G needle for single cell suspension and filtered through 40 μm nylon mesh. After centrifugation, cells were treated with ACK buffer for 5-10 minutes on ice. The mouse lineage depletion kit and AutoMACS from Miltenyi Biotec (Bergisch Gladbach, Germany) were used as directed to remove lineage positive cells after cell number determination. The lineage negative cells were treated with FC block (0.5ul/10^6) for 10 minutes on ice and combinations of antibodies for mouse Sca-1(PE-Cy7), c-Kit (APC), CD150 (Pacific Blue), CD48, Ter119,

Gr-1, B220, CD3, CD4, CD8 (PE or FITC according to the donor mice type) from BD science (Franklin Lakes, NJ) were used to further purify SKL (Sca-1+, c-Kit+, Lineage markers negative) or SLAM-SKL (SKL CD150+, CD48-) cells respectively with BD FACSAria II cell sorter (BD bioscience).

Irradiation Damage and Stem Cell Transplantation

4-6 month old C57BL6, p-selectin knockout, osteopontin knockout, NOG and Tie2-GFP mice were given 950 Rads of whole body irradiation and subsequently transplanted by retro orbital sinus (ROS) injection 48 hours following irradiation with $3X10^3$ to 10^5 purified stem cells. Antibiotics (Enrofloxacin) were added to the drinking water during the first 2 weeks of engraftment to prevent infection.

Stem Cell Labeling with DiI or PKH26 Dye

SKL cells were harvested from UBC-GFP mice as described above. For DiI dye labeling, 50μg of DiI dye (Invitrogen; Carlsbad, CA) was dissolved with 5μl of DMF solution (Sigma-Aldrich) and further mixed with cells in 100ul FACS buffer. The mixture was incubated in 37 C for 5 minutes with occasional shaking. The vial was put on ice for 15 minutes for effective dying of the cell membrane (Figure 2-2). Cells were washed with FACS buffer 3-5 times to remove debris from the DiI dye, counted and injected into the femoral artery as described. For PKH26 dye (Sigma-Aldrich), SKL cells were washed twice with FBS free PBS and 4μM of PKH 26 dye was rapidly mixed with the cells. The mixture was incubated in room temperature for 3 minutes and an equal volume of FBS to the cell suspension was added to stop the integration of the dye. Cells were washed with FACS buffer 3 times to remove debris, counted and injected into the femoral artery as described.

Tibia Window Installment

4-6 month old mice were anesthetized with avertin (200-450mg/kg, Sigma-Aldrich). In case of the cell tracking dye experiment, pentobarbital will be used (40-85mg/kg) instead of avertin. The mouse was position in a frame using the adhesive tapes in supine position under a dissecting microscope (~10-fold magnification). The mouse skin was disinfected with betadine (or other comparable) solution. The disinfection routine was done according to the ACS policy and 3 scrub technique. A small 4-9 mm incision was made starting from the top of the tibia towards the ankle in order to expose the tibia. A sterilized drill bit attached to the Dremel tool was used to gently grind a 4-9 mm area of the tibial surface to expose the marrow under the dissection microscope. An etched 10-12mm diameter autoclaved coverslip was placed over the exposed tibia to make an airtight seal around the tibia window using cyanoacrylate glue (e.g. Vetbond or comparable). Alternatively, the open area was closed with Reflex wound clips or 5-0 Ethibond braided suture (Ethicon). During this closing process, microbeads (Cytodex; Sigma-Aldrich) soaked with SDF-1 was implanted over the tibia window in some mice.

Femoral Artery Injection

The femoral artery injection was a mean to efficiently deliver the stem cell into the imaging area. The homing efficiency of the dyed cells to the bone marrow is very low. Much fewer cells (about 1/20) can be used if cells were directly injected through the femoral artery rather than through retro orbital sinus (ROS). Following anesthesia, a unilateral ligation of the femoral artery from the caudal femoral artery side branch was performed (Figure 2-3). The vessels are approached via a 4-5mm ventral incision over the proximal hindlimb. The artery is dissected free from the femoral nerve. The artery is

temporarily ligated (ribbon knot) proximally with 6-0 Ethibond braided suture (Ethicon, Somerville, NJ) to reduce blood flow briefly. The artery below the knot toward the leg is punctured with surgical knife (0.5mm) and cells are injected using a microinjection needle stretched from a glass tube. After the cell injection, the nick made for the needle insertion will be cauterized and the knot is released. After the blood flow in the femoral artery was confirmed, 0.2ml of sterile saline is dropped into the cavity and the opening is carefully closed with 5-0 Ethibond braided suture (Ethicon).

Engrafted Cell Analysis

Animals were sacrificed from 24 hour to Day 14 after the cell injection. Bone marrow cells were isolated as described above. For some animals, bone marrow cells from the central and the endosteal marrow were separated differently. For the isolation of endosteal marrow, bones were flushed as described above and the marrow-depleted bones were ground in a mortar and pestle in PBS with 1% FBS. The bone fragments were washed twice, filtered through a 40-μm filter and incubated in 5 ml of 3 mg/ml Collagenase I (Roche Diagnostics, Basel, Switzerland) and 4 mg/ml Dispase II (Roche Diagnostics) in a shaking incubator (37°C; 250 rpm for 5 minutes). The bone fragments were then washed in PBS with 1% FBS by vigorous shaking and filtering through a 40-μm filter. Both cell population was treated with ACK buffer on ice for 5-10 min to remove red cells. For the peripheral blood, samples were acquired though the saphenous vein of the cheek using a 5.0mm GoldenRod animal lancet (MEDIpoint, Inc. Mineola, NY). The blood was collected (5-8 drops) in a 5mL falcon tube (Fisher Scientific) containing 0.5 mL of 1X D-PBS and 5mM ethylenediaminetetraacetic acid (EDTA; FisherBiotech. Fairlawn, NJ) to act as an anticoagulant. The erythrocytes and granulocytes were removed using Ficoll-PLUS (Amersham Biosciences. Uppsala, Sweden) purification.

For spleen mononuclear cells, the spleen tissue was minced into small pieces using surgical scissors, passed through 18G and 20G needle in FACS buffer to make a single cell. Cells were filtered with a 40-µm filter and incubated in ACK buffer for 5 min on ice. After the cell number determination, cells from bone marrow, bone, peripheral blood and spleen were resuspended into FACS buffer and the same antibodies for cell sorting was used to analyze the fate of the engrafted stem cells using BD FACS Canto II (BD bioscience).

In Vivo Imaging

In vivo fluorescent imaging was performed directly after cell delivery, while the animals were still sedated. Images and videos were acquired at 5-20X magnification using LEICA DM5500B microscope, a Hamamatsu 3CCD camera and Volocity 4.3 software (Improvision). During the in vivo imaging step (initial observation is usually done 4-72h after tibia window installation), the mouse was put on a disinfected stage specially designed for the microscope use. The skin was disinfected with betadine using a 3 scrub technique. In case the suture or clips were used, they were carefully removed. After the observation under the microscope, the exposed area was closed with the sutures or clips and plastic bandage was applied around the leg to prevent damages.

Magnetic Resonance Imaging of HSC

MRI was performed at 17.6T (750MHz) magnetic field strength following transplantation (Bruker BioSpin, Madison, WI, USA) using Paravision 4.0 software (Bruker, Madison, WI, USA). Animals were anesthetized during the imaging process by breathing a mixture of isofluorane and oxygen. Respiration and body temperature was monitored during the imaging process (SA Instruments, Stonybrook, NY, USA). A custom-built single tuned 8X11mm^2 surface coil (Doty Scientific, Columbia, SC, USA)

was placed over the knee and tibia, allowing imaging of the BM space. 3D gradient echo scan sequences were obtained with imaging parameters of: repetition time (TR)= 80ms, echo time (TE)= 2.5ms, field of view (FOV)= 1.1X0.6X0.5cm^3, matrix size= 393X 214X83, spectral width= 75kHz and four signal averages, resulting in an acquired resolution of 28X28X60mm^3, which was later zero-filled to 21.5X23.5X39mm^3 for image presentation.

Perfusion of the Animal

To preserve microstructure of the tissues, 4% PFA was perfused to some animals before tissue collection. The mouse was given an IP injection of Avertin (300-400mg/kg) to reach a deep state of unconsciousness, as determined by the abolition of the toe pinch or pedal reflex test. The incision area was wetted with ethanol and the chest cavity was opened using surgical scissors from the diaphragm to above the heart, being careful to avoid cutting any large blood vessels. Once the chest cavity was open and the heart exposed, the ribs and connective tissues were incised around the heart. While the heart was still beating, it was punctured at the left ventricle with an 26-gauge needle (5mL syringe containing 5mL of 4% paraformalydehyde in phosphate-buffered saline). The right atrium is punctured with another 26-gauge needle and perfusion started at a rate of 5 mL/minute until the entire volume is depleted. The organs of interest are immediately removed. Death is assured via the de facto thoracotomy involved in heart exposure.

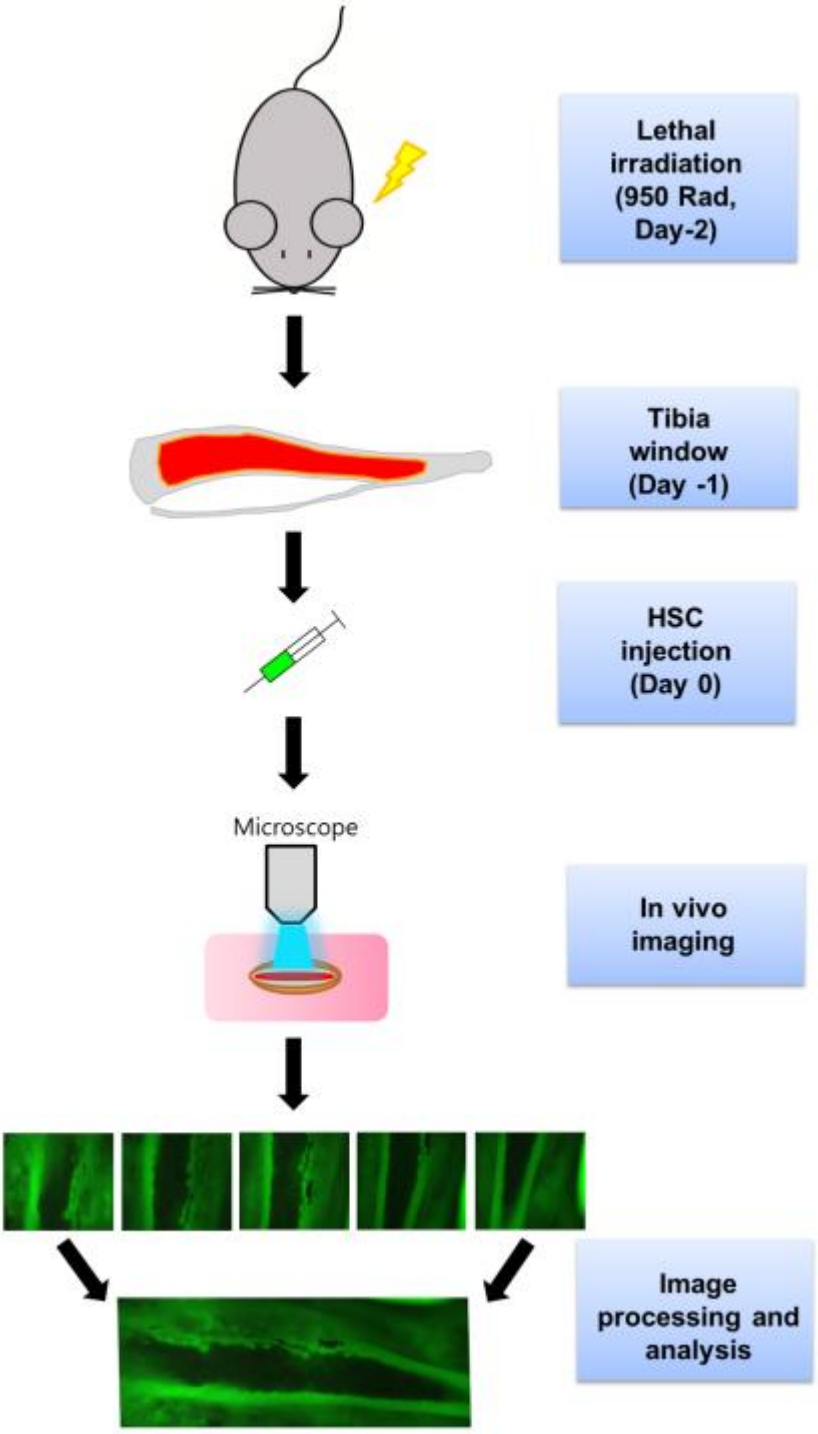

Figure 2-1. Overview of the tibia window method.

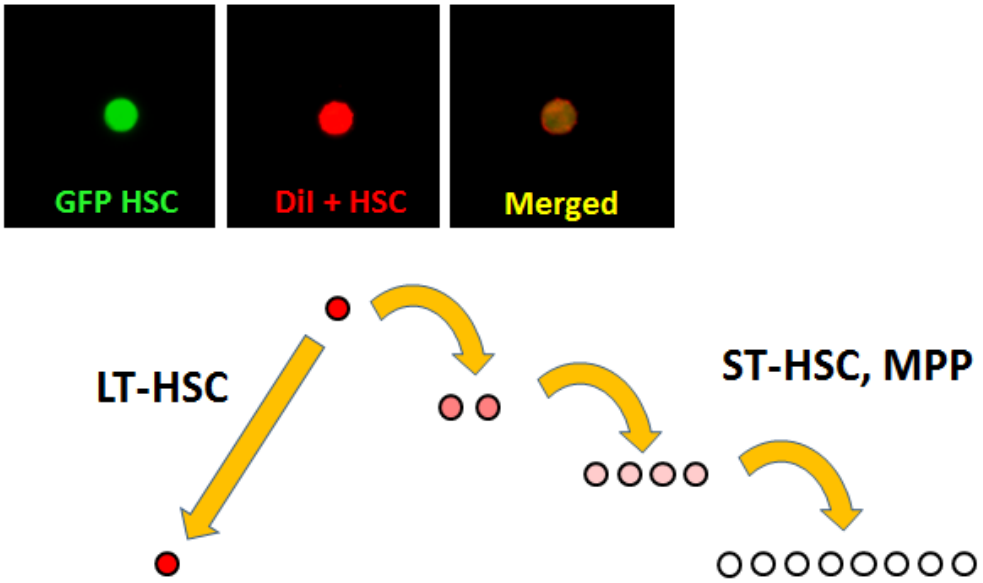

Figure 2-2. A representative image of the DiI dye stained GFP+ SKL cell. Long term HSC (LT-HSC) tends to retain the cyanine dye while dyes in short term HSC (ST-HSC) and multi-potent progenitors (MPP) are rapidly diluted after cell division.

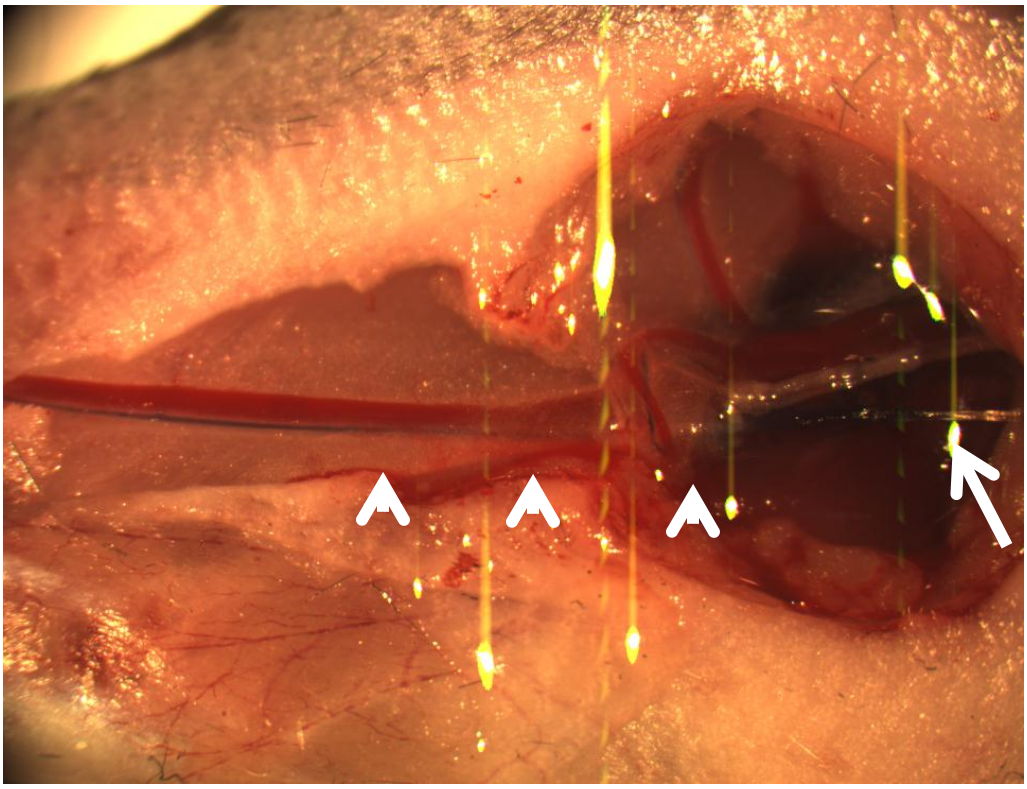

Figure 2-3. An image to highlight the femoral artery. The femoral artery (arrow heads) was stained with Evans Blue dye. The arrow indicates the cell injection site.

CHAPTER 3
IN VIVO IMAGING OF THE HSC ENGRAFTMENT USING THE MOUSE TIBIA WINDOW MODEL

Introduction

Traditionally, HSC studies have been focused on in vitro experiments such as colony forming assays and in vivo functional assays such as bone marrow rescuing by HSC transplantation (65). The limitation of the previous studies is that it assessed the ability of cells to proliferate in specific in vitro culture conditions and/or it is only a surrogate for testing HSC self-renewal ability. Bone marrow transplantation is the gold standard experiment to test HSC function in vivo, but the stem cell population injected is not a homogeneous stem cells. They are the mixture of the different stem and progenitor cells and reconstitution of the BM may only be achieved by a small portion of the true stem cell. As the ability to reconstitute bone marrow and peripheral blood of lethally irradiated recipient mice is only end point readout, it is not clear which cell type actually repopulated the BM. Therefore, this approach does not allow us to analyze what cell type is engrafted and what is happening during the engraftment and repopulation process. Moreover, it takes many months to make sure stem cell progeny is established and repopulated. During the experimental period, aside from periodically collecting blood samples for peripheral blood analysis, little information is learned about the transplanted HSC (64). In the experimental model described here, I aim to monitor the very early stage of the engraftment process and the repopulation pattern of the engrafted cells in the BM.

In Vivo Tracking by Using the Tibia Window Model

Dr. Ed Scott and I have developed a method called the tibia window to track fluorescent cell HSCs in the tibia of living animals. This application is described in figure

2-1. Briefly, after the lethal irradiation, the tibia bone was exposed and the surface of the bone was ground by a surgical drill until the inside bone marrow can be clearly visualized (20-80um thickness, Average 42um Fig. 3-1). Imaging was done in living mice using fluorescent and confocal microscopes which did not alter their viability, did not interfere with hematopoietic reconstitution, and could easily be used to follow the temporal dynamics of hematopoietic reconstitution in a living mouse (62-64). Using this imaging system, we studied the topologic and temporal patterns of recruitment, proliferation, and seeding of hematopoietic cells enriched in HSCs in the tibial bone marrow after lethal irradiation. As shown in figure 3-2 and 3-3, tibia window can deliver superior images at the single cell level for longer period of time compared to other current real-time imaging techniques (20, 62-64). By using this model, I aimed to define the mechanisms that regulate the recruitment and initial proliferation of hematopoietic cells in mouse bone.

SKL HSC Engraftment in the Osteoblastic Niche

In vivo imaging of the mouse tibia bone suggested that the osteoblastic niche is the most active area for SKL HSC population not only to engraft but also to proliferate. As shown in figure 3-2, most bright colonies developed after stem cell injection located near the bone which suggests that the osteoblastic niche would be a better place for stem cell lodgment and proliferation. However, not all endosteal surfaces seem to be sufficient to act as the osteoblastic niche since some cells that were engrafted on the endosteal surface failed to develop into the clusters or the colonies in the tibia window (Fig. 3-3 E-I). Several reports emphasize the importance of the interaction between osteoblasts and the HSC in the HSC niche (33-45). Critical factors secreted from the osteoblast include angiopoietin, osteopontin, steel factor and CXCL12 and the binding

molecule N-cadherin or extracellular matrix can also greatly affect HSC in proliferation, quiescence and survival (57, 58, 63). Ex vivo imaging is another benefit of the tibia window. Usually, 5-10X magnification lenses are used for in vivo imaging as >20X magnification required water lenses and it is very difficult to get quality images in living animal. However, the tibia bone can be harvested, fixed in 4% PFA and imaged using high power magnification in a confocal microscope for better resolution. Ex vivo imaging in the tibia window also shows that the proliferating HSC colonies are formed on the osteoblastic niche (Fig. 3-4A). In contrast, cells engrafted in the vascular niche was scattered and rarely formed colonies even at D5 and after (Fig. 3-3B). Higher magnification of a single engrafted HSC indicates the possible interaction between the osteoblasts and the HSC (Fig. 3-3 C,D). 3D rendering of the tibia bone is shown in Fig. 3-4 and the use of RGB filter was beneficial as the researchers can clearly distinguish autofluorescence from the bone from the true signal originated from the engrafted cells.

In Vivo Imaging with Different Cell Types and Microbeads

Although the detailed engraftment event can be observed with the tibia window, it is a highly invasive model due to the opaqueness of the bone. Therefore, validation of the method is critical to make sure that what was observed was not from bone grinding or the surgery itself. The main characteristics of the HSC are self-renewal and differentiation. Upon engraftment on lethally irradiated mice, the HSC located on the niche start to divide and rapidly expand to make up the damaged BM cells. To observe the difference of behavior between HSC and mature blood cells, $6X10^5$ lineage positive cells were injected into the mice with tibia window (Figure 3-5). The number was 20 times more compared to the injected HSC ($3 X10^4$ SKL cells) but until Day 5, few cells were observed in the tibia window and cells were scattered all over the area. In addition,

none of the observed cells divided or formed colonies. This should be due to the lack of homing and lodgment mechanism in mature blood cell. Next step, I decided to test the CD133+ myeloid progenitor population. This time, two populations with different color ($3X10^4$ SKL cells from GFP mice and $6X10^5$ CD133 positive cells from DsRed mice) were injected together into mice with the tibia window to highlight the difference of stem and progenitor cell behaviors in the BM. As shown in Figure 3-6, CD133+ progenitor cells were observed as well as SKL cells, but they did not proliferate to form colonies in any BM cavities which suggest that only the HSC derived from SKL population has the ability to engraft and repopulate the BM. I further validated the tibia window by implanting the CXCL-12 soaked microbead onto the center of the tibia window to know whether I can modulate the niche (Figure 3-7). As shown in introduction, CXCL-12 or SDF-1 is the critical soluble factor in the bone marrow with the gradient toward the osteoblastic niche (48). Figure 3-7 D and E show that the HSC are attracted by this external CXCL-12 gradient and formed a colony on the microbead.

The Relationship Between the Two Niches

One benefit of the non-invasive imaging techniques such as CT or MRI is that it can remain the subtle microvessel structure in the microenvironment intact compared to invasive imaging approach. Since the BM is filled up with microvessels, I used Tie2-GFP mice to make sure the endothelial cells on the tibia window surface are normal. Tie2 is expressed in all endothelial cells including the BM sinusoid cells and the result indicated that the bone grinding process in tibia window model left the BM vessel undamaged (Figure 3-8). The lineage negative cells from DsRed mice were injected into the Tie2-GFP mice with the tibia window to demonstrate that the circulating cells before the engraftment could be observed using the tibia window. Compared to the lineage

positive cells, the lineage negative cells continuously changed shapes moving much more slowly along the sinusoid and the time that cells were attached to the endothelium was much longer. Figure 3-9 shows that the colonies developed on the osteoblastic niche were also covered with the sinusoid (perivascular niche), which suggest the two niches cannot be distinguished from each other on the endosteal region. Indeed, endothelial cells also secrete many important factors such as angiopoietin 1 to manipulate the HSC (46-51). The close location of the osteoblastic niche components and the vascular niche components may have synergistic effect to the engrafted HSC.

Non-invasive MR Imaging

As I wanted to further confirm what I have observed using non-invasive imaging technique, MR imaging was done to the mice injected with HSC labeled with Feridex. The basic experimental design was to administer theoretically equivalent numbers of HSC as either Feridex-labeled WBM or Feridex-labeled SKL-enriched HSC. Using short echo time, high resolution 3D MRI, acquired for 48h or longer post-transplant, I was able to detect multiple clusters of Feridex-labeled donor cells as small regions of signal void located throughout the tibia (Figure 3-10). These areas of signal void, corresponding to the previously observed fluorescent cell clusters, measured approximately 80–110nm in diameter. Dataset analysis showed that donor cell engraftment occurred at an average distance of 132±102 um distance from the edge of the calcified bone 48h post-initial transplant. This distance is within five cell diameters of the bone, which is highly supportive of engraftment of the endosteal niche. However, the engrafted cells marked with Feridex could not be observed after 72h post-transplant time frame primarily by signal loss due to Feridex label dilution from cell division. Although I could not observe events after 72h, the results from MRI also suggested that

a limited number of available engraftment niches exist only within the endosteal surface.

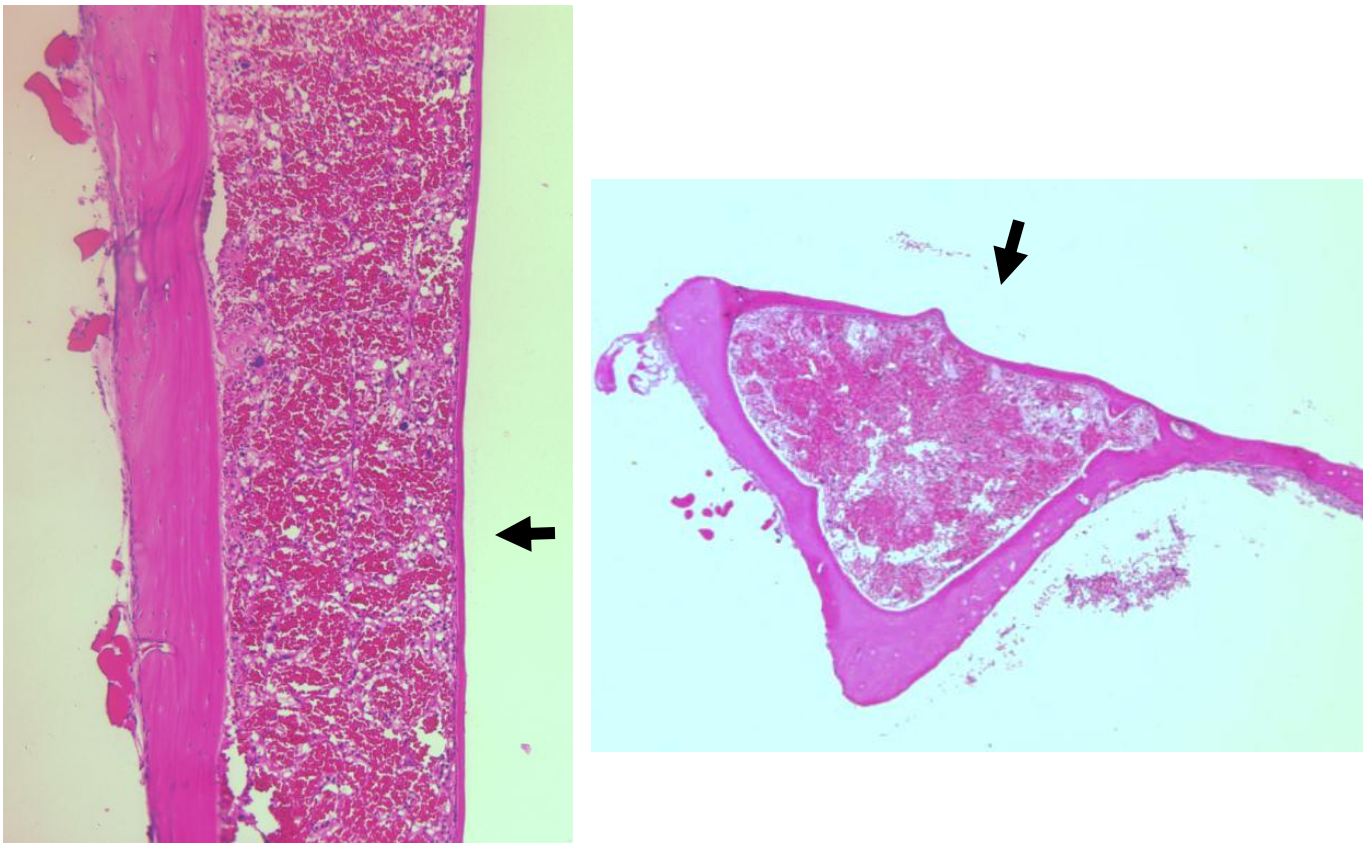

Figure 3-1. Hematoxylin and eosin staining of the tibia. Arrows indicate the observation area under the upright microscope. Average thickness of the window was 42 micrometer.

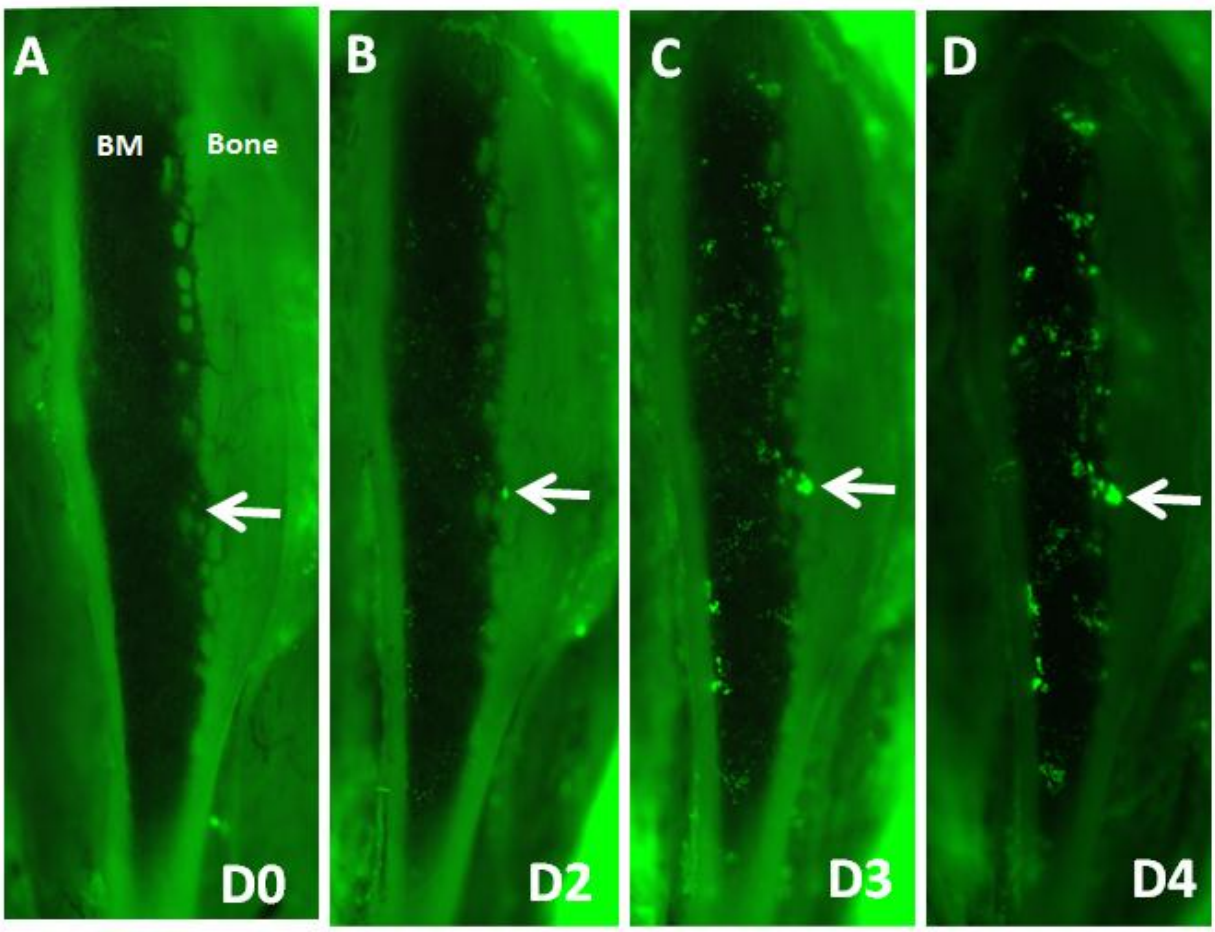

Figure 3-2. In vivo imaging of the tibia window in a representative C57BL/6 mouse. [A-D] Low magnification mosaic images to display engraftment process in the whole tibia region. Arrows are to mark the same area and to indicate a developing colony originated from the osteoblastic niche. [E-I] Higher magnification of the arrowed area showing detailed engraftment process occurred in the osteoblastic niche. Yellow arrow heads indicate the area HSC failed to engraft.

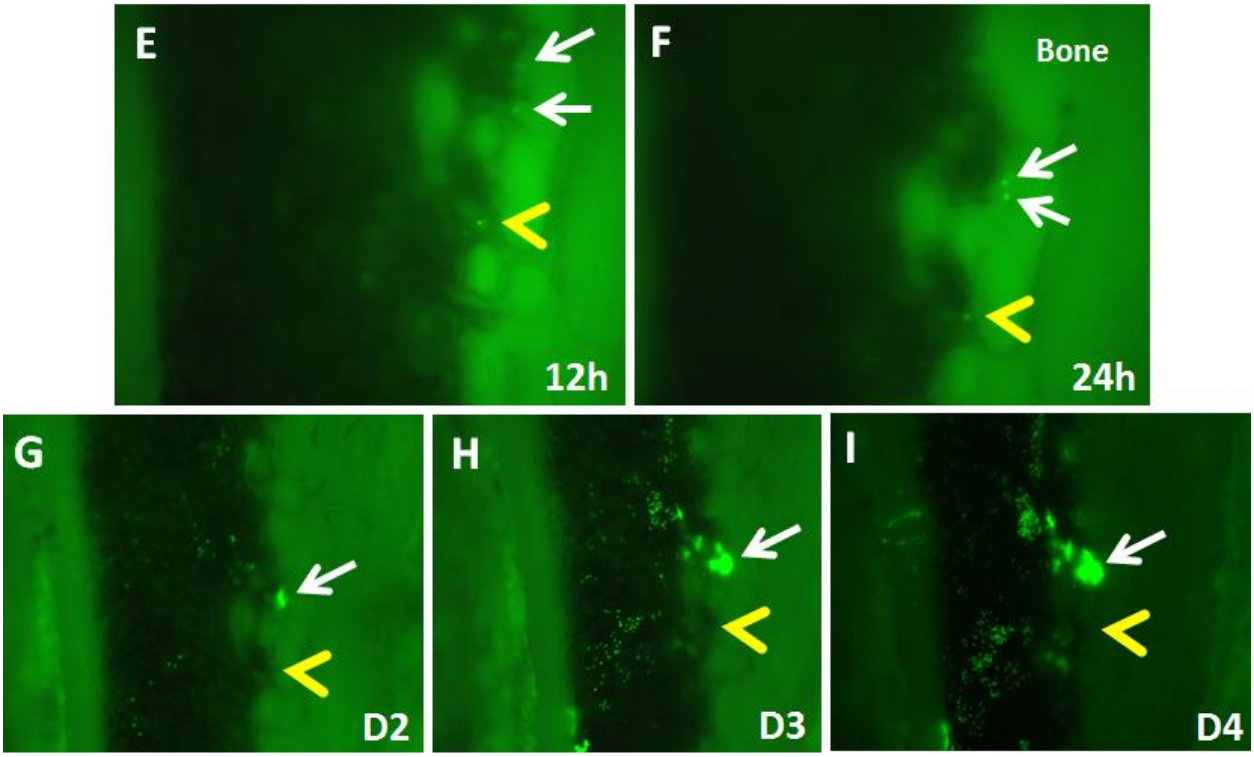

Figure 3-2. Continued.

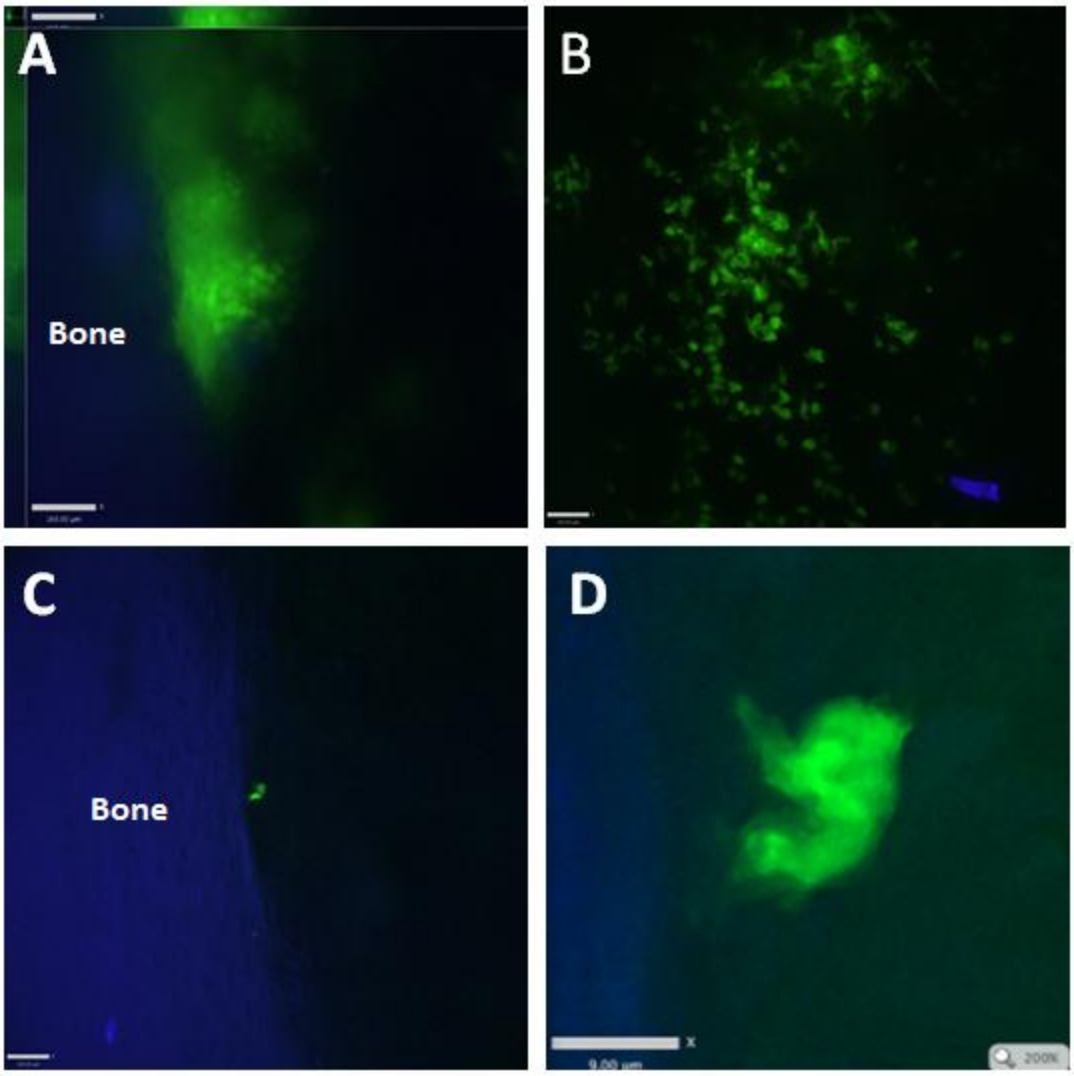

Figure 3-3. Ex vivo imaging of the HSC engraftment in the mouse tibia window. [A] 3D confocal image showing a SKL HSC derived colony formation in the osteoblastic niche at day 4. [B] Typical engraftment pattern in the perivascular niche. [C-D] Low and high magnification of the engrafted SKL HSC in the osteoblastic niche. The magnification was 10X and 63X respectively.

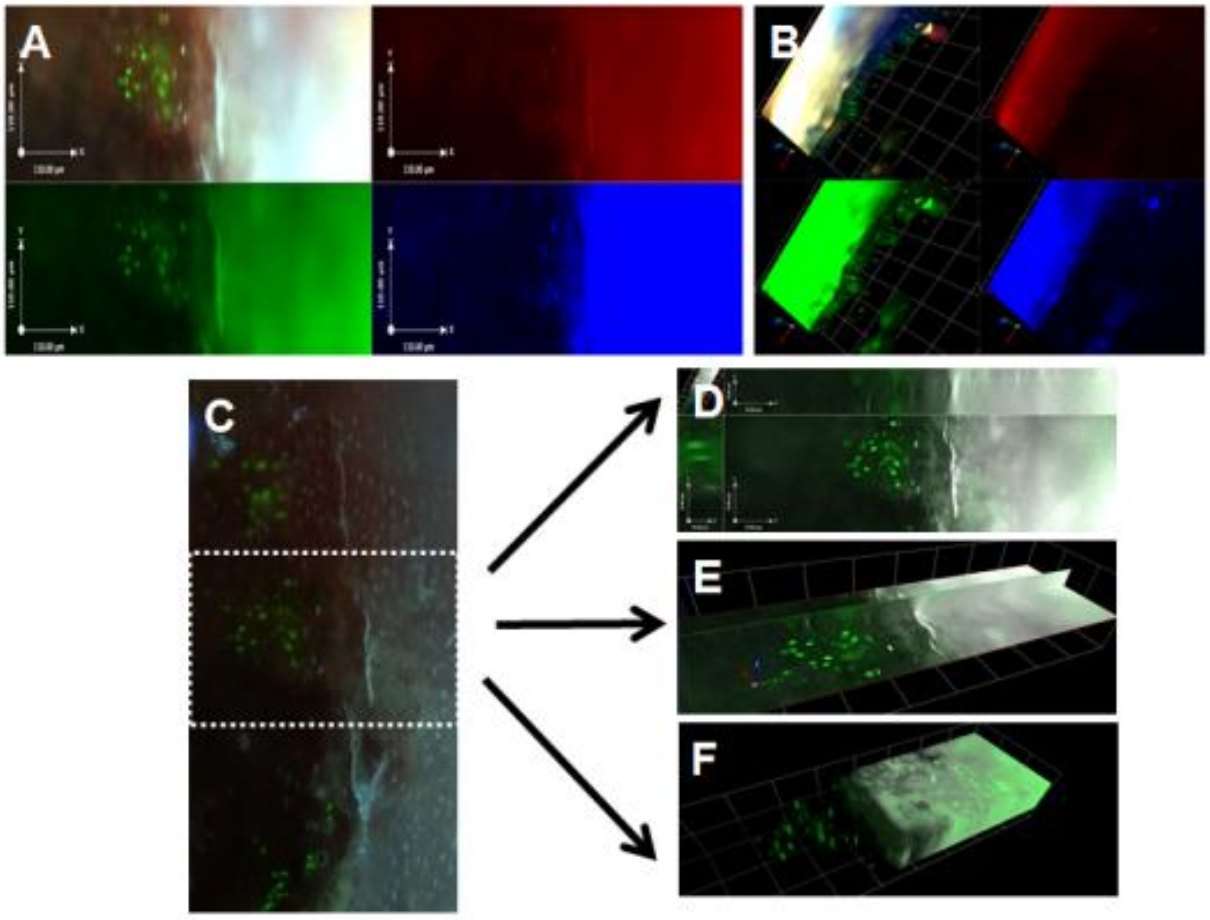

Figure 3-4 Usage of the RGB filter and 3D rendering process in tibia windowed animals. [A] Use of RGB filter to highlight the bone structure and GFP positive cells.Bone is highly autofluorescent and the RGB filter clearly separate bone tissue and GFP positive stem cells. [B] Z-stacked image using RGB filter. [C, D] Image process to reconstitute 3D image in live animals.

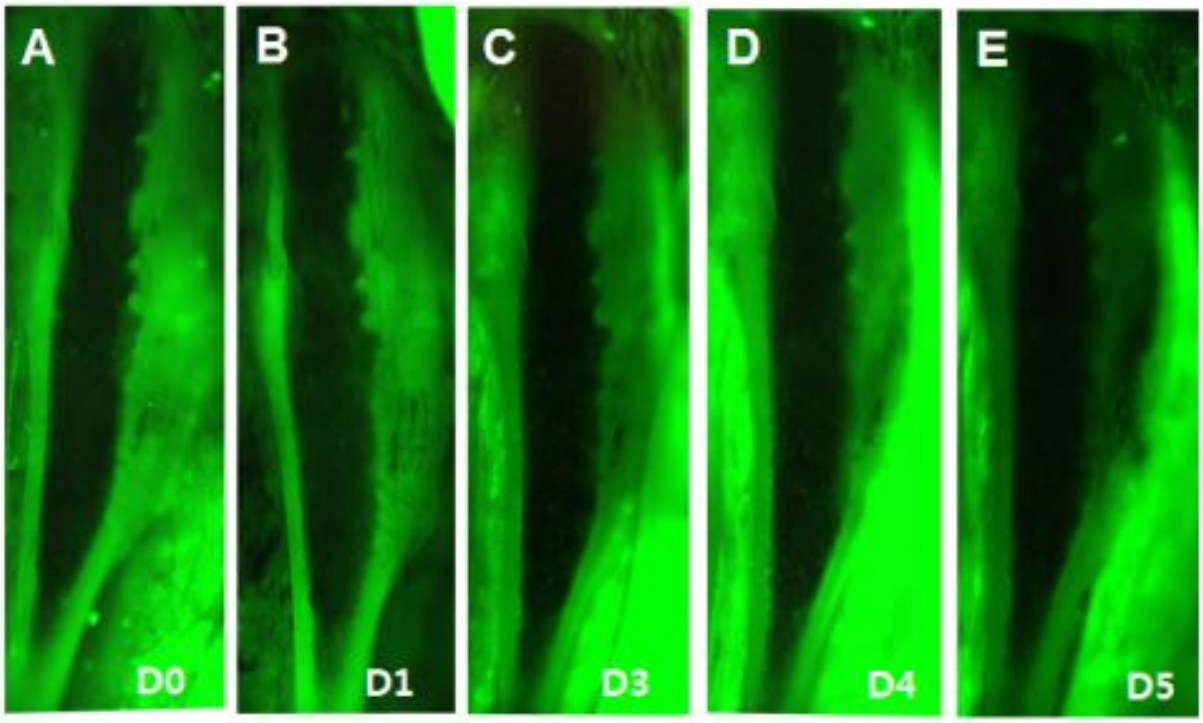

Figure 3-5. An animal injected with $6X10^5$ lineage positive cells. Although 20 times more cells were injected compared to SKL cell injection, few cells were observed in the tibia window imaging and none formed any colonies.

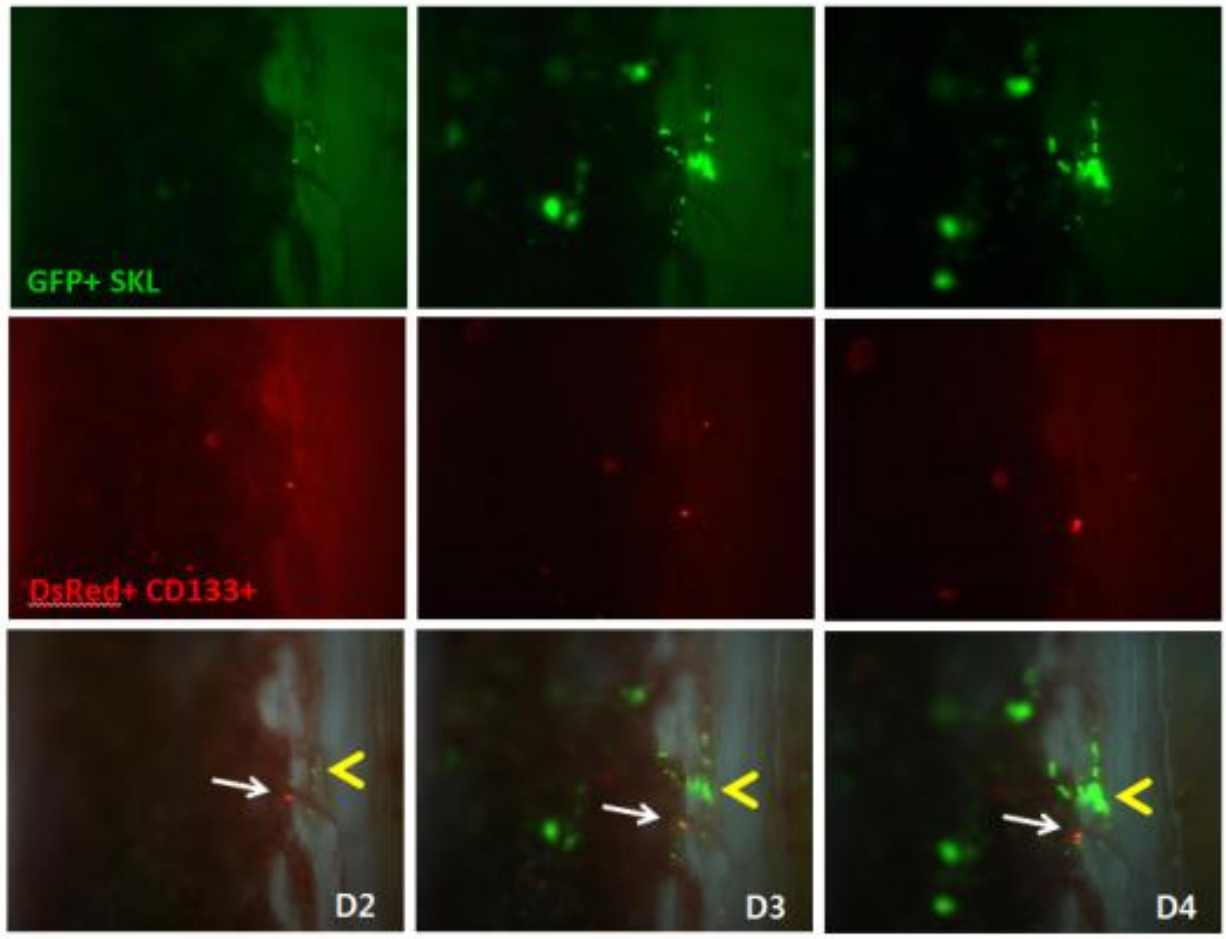

Figure 3-6. An animal injected with $3X10^4$ SKL cells from GFP mice and $6X10^5$ CD133 positive cells from DsRed mice.CD133 cells were significantly fewer in the tibia window and did not proliferate or formed colonies (white arrows). In contrast, SKL cells were actively engrafted near the endosteal region and formed several colonies (yellow arrowhead).

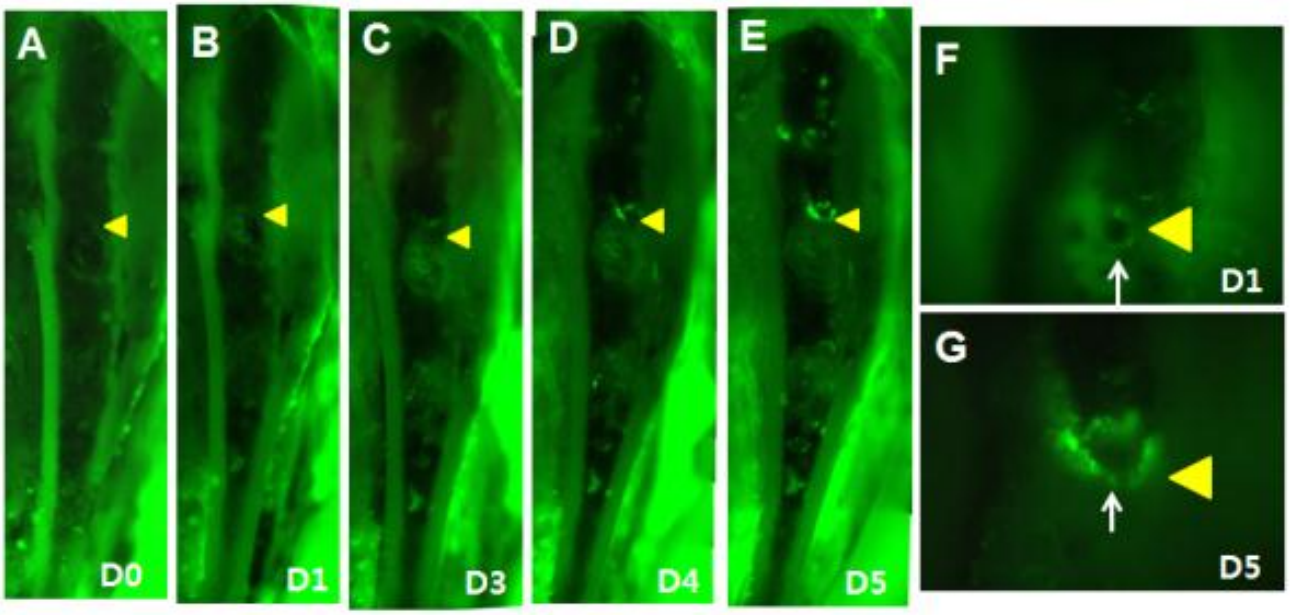

Figure 3-7. Tibia window with 0.5 ng/μl of SDF-1 soaked microbead. [A-E] Mosaic images of the tibia window from day 0 to day 5. Additional 0.5ng of SDF-1 was added to the microbead (yellow arrowhead) at day 1. {[F-G] SKL cells were recruited to the SDF-1 soaked bead and formed a colony.

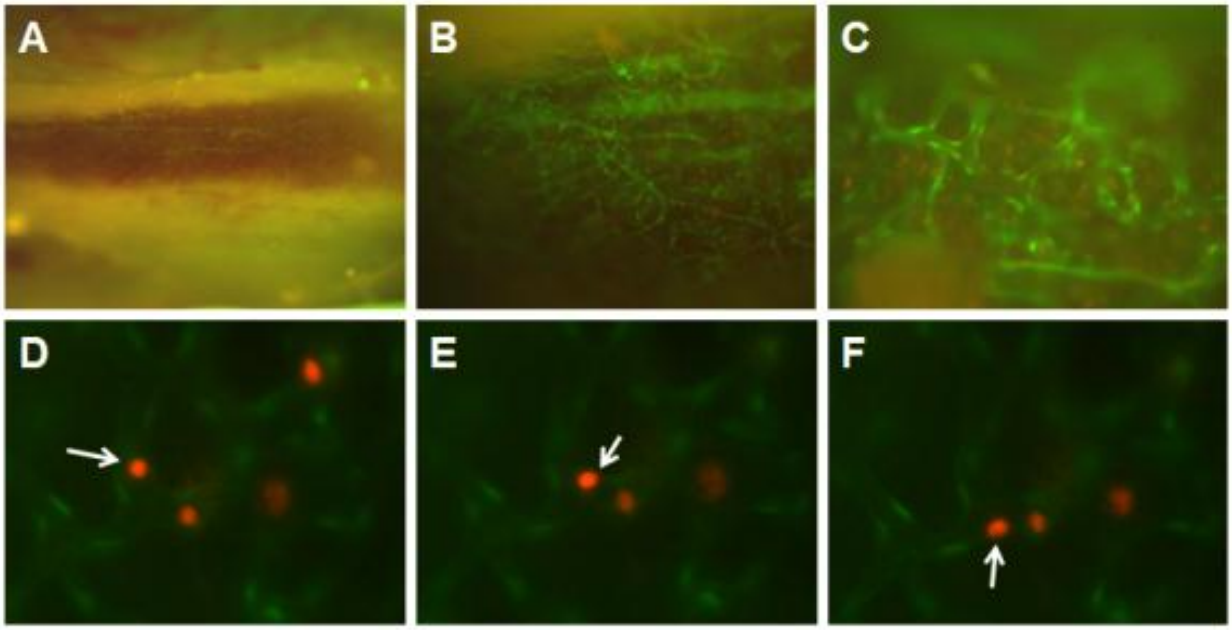

Figure 3-8. In vivo imaging of the tibia window in a Tie2-GFP mouse. [A-C] Low to high magnification images to display intact bone marrow microvasculature after tibia window. [D-F] Lineage marker negative DsRed cells were injected into the Tie2-GFP mice. Arrows are to mark the same cell circulating in the sinusoid. Note that the rolling cell is in contact with the endothelium and continuously changes shapes.

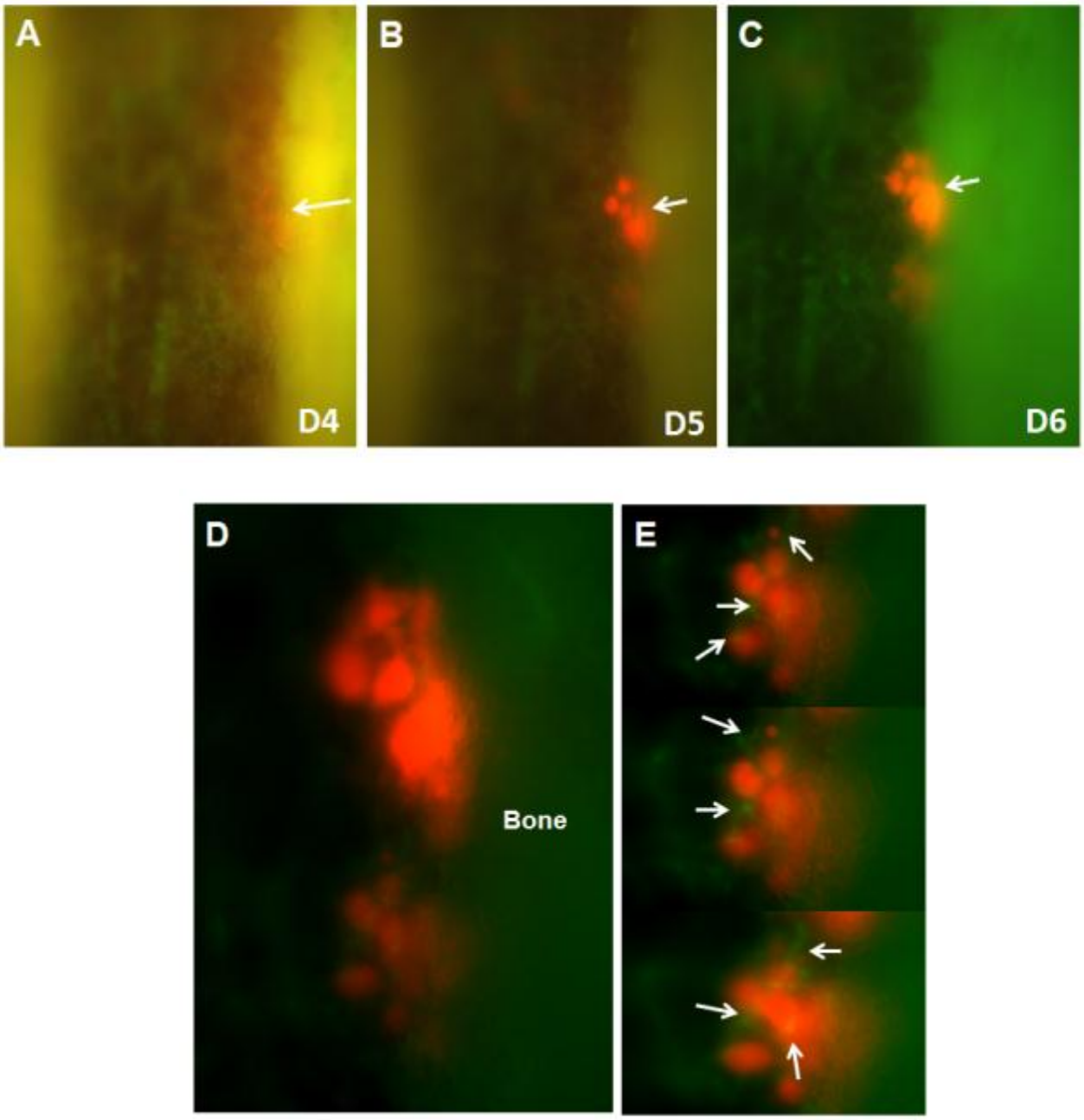

Figure 3-9. Engraftment of the DsRed positive SKL cells in the Tie2-GFP mice. [A-C] As observed in the B6 mice, DsRed postivie SKL cells were also engrafted mainly on the osteoblastic niche. [D-E] Higher magnification (20X) and Z-stacked images indicates that the osteoblastic niche is very well vascularized (arrows).

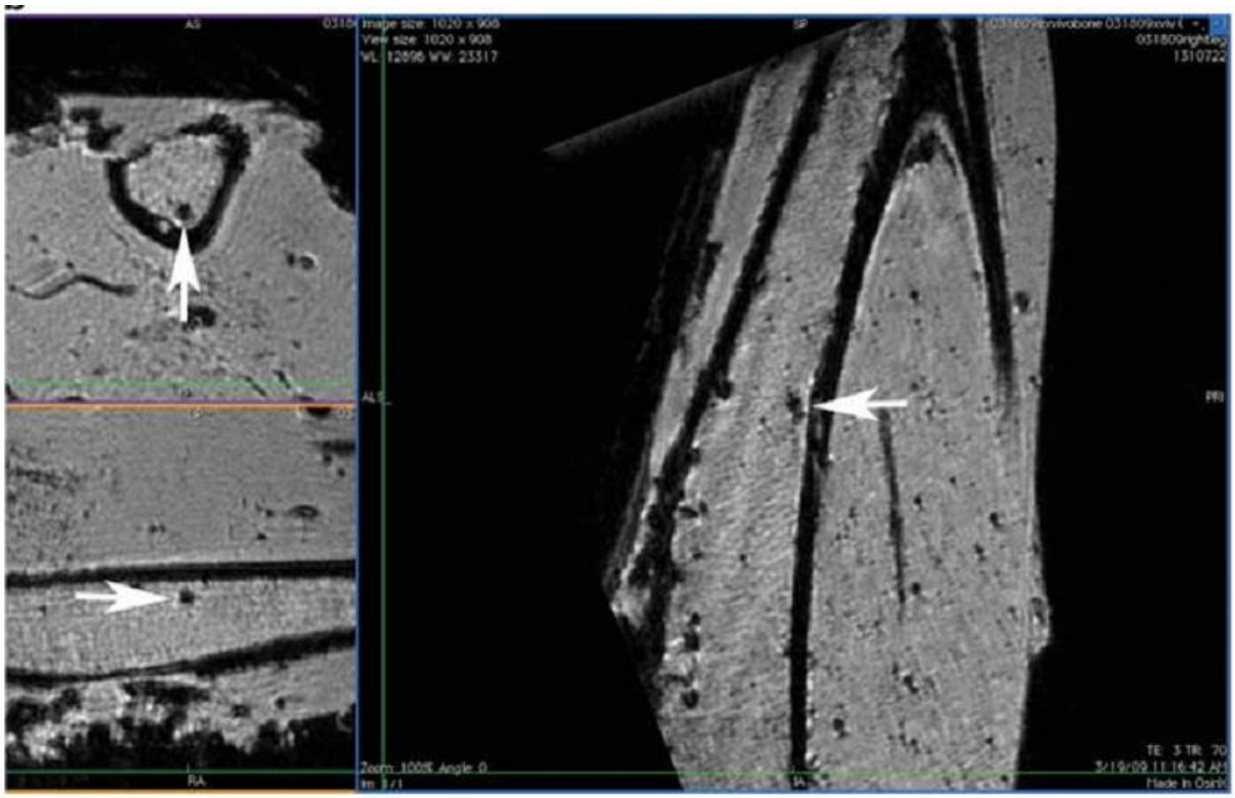

Figure 3-10. MRI image of the GFP+ SKL cells coated with Feridex 48 hours after transplantation. SKL cells are located near the endosteum (arrow). Non-invasive imaging techniques such as MRI also confirms what was observed in the tibia window model.

CHAPTER 4
ROLE OF THE MICROENVIRONMENT IN THE HSC ENGRAFTMENT PROCESS

Introduction

There are a lot of suggestions in the literature about the nature of the hematopoietic stem cell niche (53). Over the past several years the most popular model in the literature has been the idea that hematopoietic stem cells reside in the osteoblastic niche (33, 36-42). The osteoblastic niche is the most popular model of which held that hematopoietic stem cells adhere by N-cadherin-mediated homophilic interactions with osteoblasts and osteoblasts secrete all the factors that regulate stem cell maintenance (36, 63). There are papers in the literature that interpret their data through the prism of the osteoblastic niche model. However, many critical elements of that model had never been tested directly. Osteoblasts may directly or indirectly regulate hematopoietic stem cell maintenance through several mechanisms that don't necessarily involve cell-cell contact. There are a lot of data that's emerging from many laboratories, suggesting the possibility of a perivascular niche in bone marrow. However it is also hypothetical because the almost all region of the BM is vascularized and nobody has yet conditionally deleted any critical niche cell type in the bone marrow, nor depleted factors that are genetically required for stem cell maintenance. Therefore, all of the arguments remain somewhat indirect in terms of the identity of the niche. And that's why experiments are required using various knockout mice and different types of HSC population.

HSC Engraftment in the Normal Physiological State

The bone marrow microenvironment is rapidly and dramatically changed by the irradiation procedure (66). Therefore, it is important to understand the HSC engraftment

or homing process in normal physiological condition. As the engraftment of the HSC in C57BL/6 mice without lethal irradiation does not occur efficiently, I used NOG mice, an immune compromised mice strain that can accept HSC even from human without any irradiation (Figure 4-1). Even though the engraftment and the colony formation happened in the osteoblastic niche like C57BL6, there were differences in engraftment without the irradiation in NOG mice. At first, the cell number observed in the tibia window was much fewer in NOG mice while almost twice the number of the SKL cells was injected compared to C57BL6 mice. Secondly, many of the cells that found in the osteoblastic and perivascular niche did not proliferate actively. These observations could be because there is no strong homing or proliferating signal for the transplanted HSC or fewer available niches for HSC to engraft in normal physiological state.

Quiescent HSC in the Osteoblastic Niche

Most primitive HSCs are quiescent (36, 67). Using DNA label BrdU and H2B-GFP incorporation respectively (14), LT-HSC were found to be predominantly located in the endosteum and subsequently confirmed to be a primitive HSC population (8, 9, 38, 68). The quiescent HSCs have superior long-term reconstitution potential. However, HSCs in this population cycle only once every 145 days on average and thus may not provide ongoing support for production of billions of blood cells, although they can be activated for this function under injury conditions (9).

Here, the DiI and PKH26 dyes are used to trace the location of the LT-HSC (Figure 2-2). Since the dyes only exist in cell membrane, the intensity of the signal becomes half with every cell division. As explained in Chapter 2, the stained cells were injected through the femoral artery due to delivery efficiency. I could observe the dye retaining cells that were located on the osteoblastic niches on day 3 (Figure 4-2).

However, no cells with the dye were found after the cell division in the central marrow region with the dye signal, which is consistent with previous reports (28). The result from the histology also matched what was observed in the tibia window (Figure 4-3 A and B). Next, the BM cells from the central marrow region and the endosteal region were separately purified and analyzed with FACS for DiI or PKH26 dye signal (Figure 4-3 C and E, the method described in Chapter 2). There was 10 times more dye retaining cells in the BM population from endosteal surface, which again confirmed the event that was observed in the tibia window.

Aberrant HSC Engraftment in P-selectin Knockout Mice

Along with other cell adhesion molecules, P-selectin involves in many critical steps during hematopoietic cell rolling and tethering on endothelial cells. In addition, FACS results showed that 99% of the SKL HSC population expresses the P-selectin receptor PSGL-1 (P-selectin glycoligand 1; Fig. 4-4). In order to investigate the importance of this molecule, P-selectin knockout mice were used. When SKL cells were injected into the tibia window installed mice, most of the engrafted cells were observed in the central marrow region which is very different from what was observed in the normal C57BL/6 mice (Fig. 4-5). Interestingly, the cells engrafted in the vascular niche proliferated and formed small clusters around the vascular niche. Although none of them grew bigger to be called as a colony derived from HSCs, it was clear that the interaction between the osteoblastic niche and the HSC is dispensable for HSC survival and proliferation. However, when compared to the cells that happened to be engrafted in the osteoblastic niche, those which engrafted in the vascular niche didn’t proliferate well (Fig. 4-5). This highlights the importance of the osteoblastic niche for efficient engraftment and proliferation process

Osteopontin as a Negative Regulator for HSC Proliferation

Osteopontin is one of the sialoprotein that is secreted by osteoblasts in the bone marrow. Osteopontin is known to repress HSC proliferation, which makes it a key component to harness the osteoblastic niche bound HSC to become quiescent. To evaluate the role of osteopontin and abnormal osteoblastic niche, we used osteopontin knockout mice. As shown in figure 4-7, HSC engrafted throughout the bone marrow space on both osteoblastic and vascular niches. As the microenvironment doesn't have the osteopontin, HSCs could also engraft in the vascular niche which suggests that osteopontin is a strong chemoattractant to HSC population. The initial engraftment pattern in histology is summarized in Figure 4-8 for both P-selectin and osteopontin knockout mice. I further wanted to know whether the aberrant microenvironment in the bone marrow also affect BM cell mobilization. To achieve this goal, I damaged the mouse eye with laser and injected 1ug of VEGF protein directly into the mouse eye to induce proliferative adult retinopathy. As shown in Figure 4-9, the eye from osteopontin knockout mice had much severe BM derived cell contribution, which circumstantially suggested that the altered microenvironment in the BM facilitated the mobilization process.

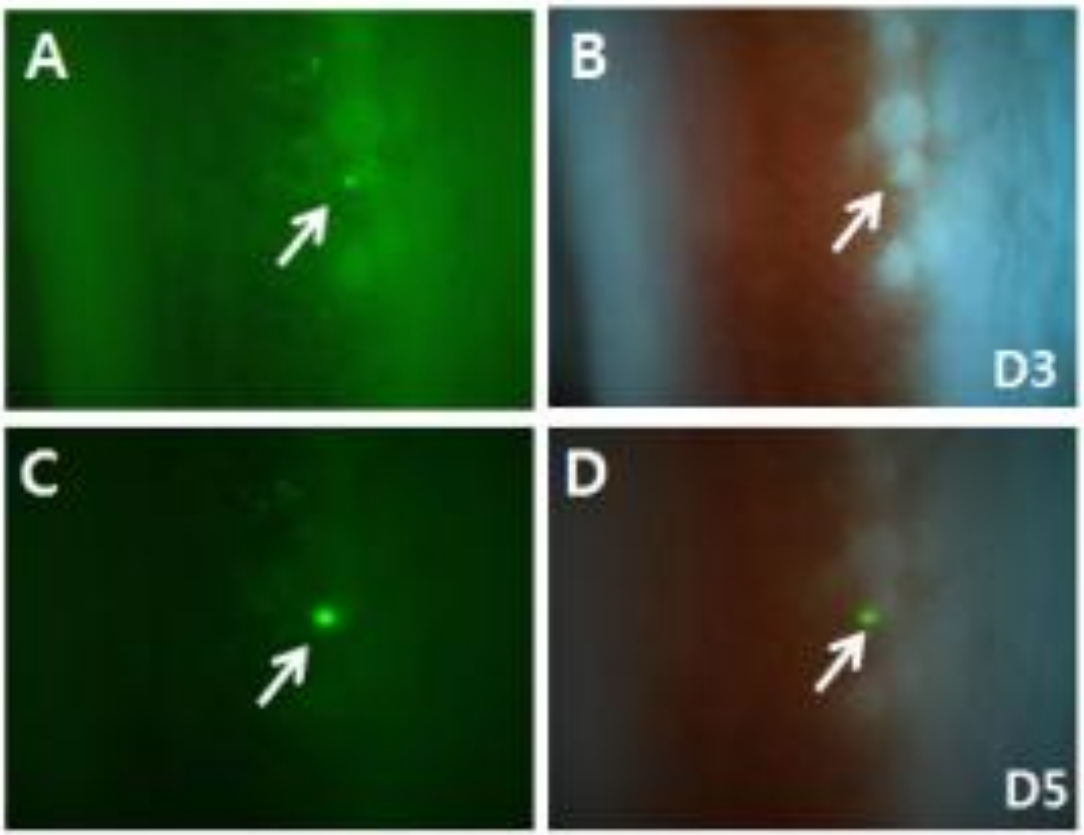

Figure 4-1. A representative image of NOG mice with $5X10^4$ GFP+ SKL cells without irradiation. [A-B] Engraftment of the HSC on the endosteum. [C-D] The engrafted cells formed a colony at Day 5. No colonies were observed in the central marrow region.

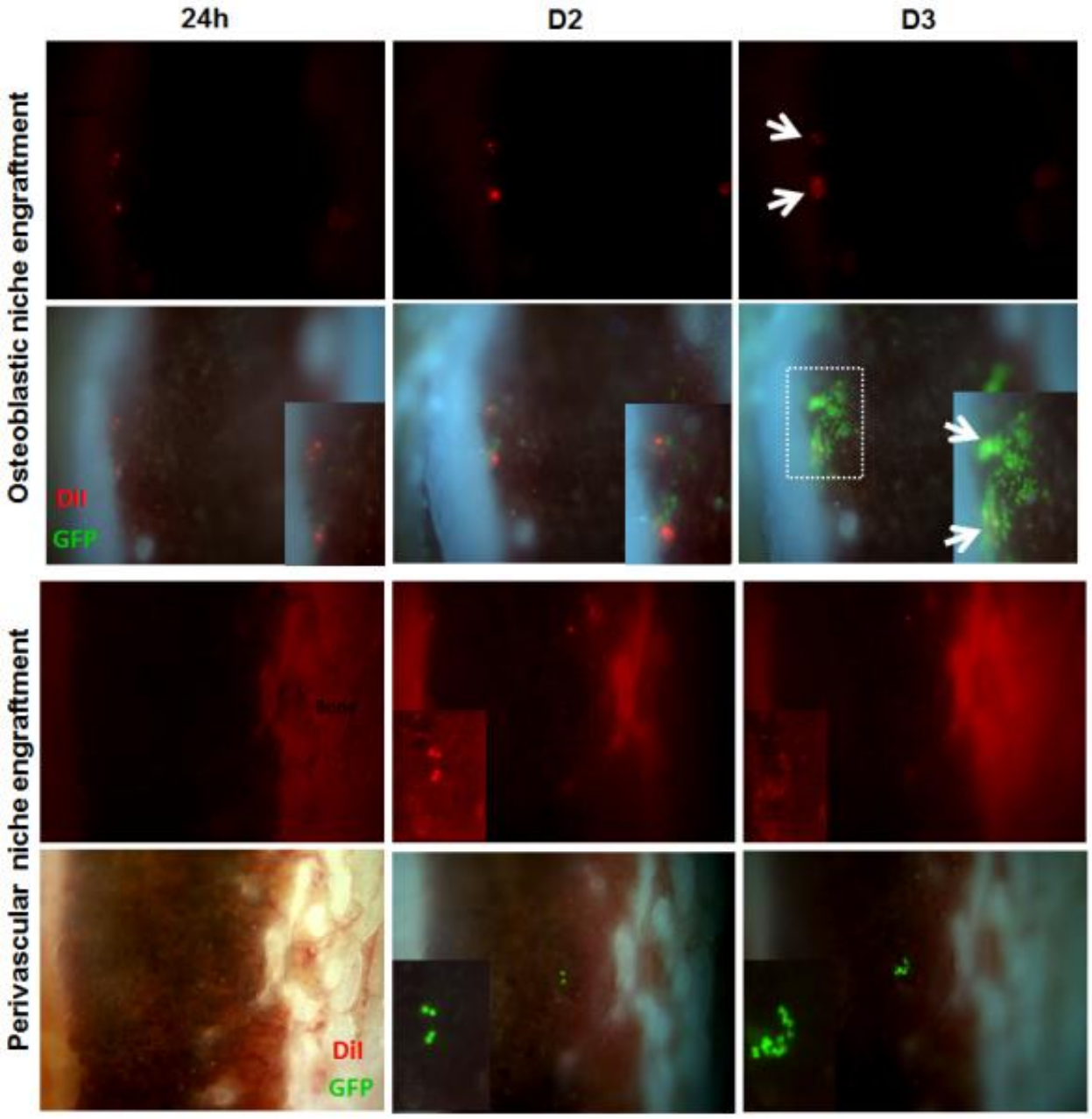

Figure 4-2. Engraftment of GFP positive SKL cells with the DiI dye. SKL cells engrafted in the osteoblastic niche retained DiI dye on the endosteal surface at day 3 (Upper panel)., In contrast, the DiI dye on SKL cells that were observed on the perivascular niche disappeared within 24 hour.

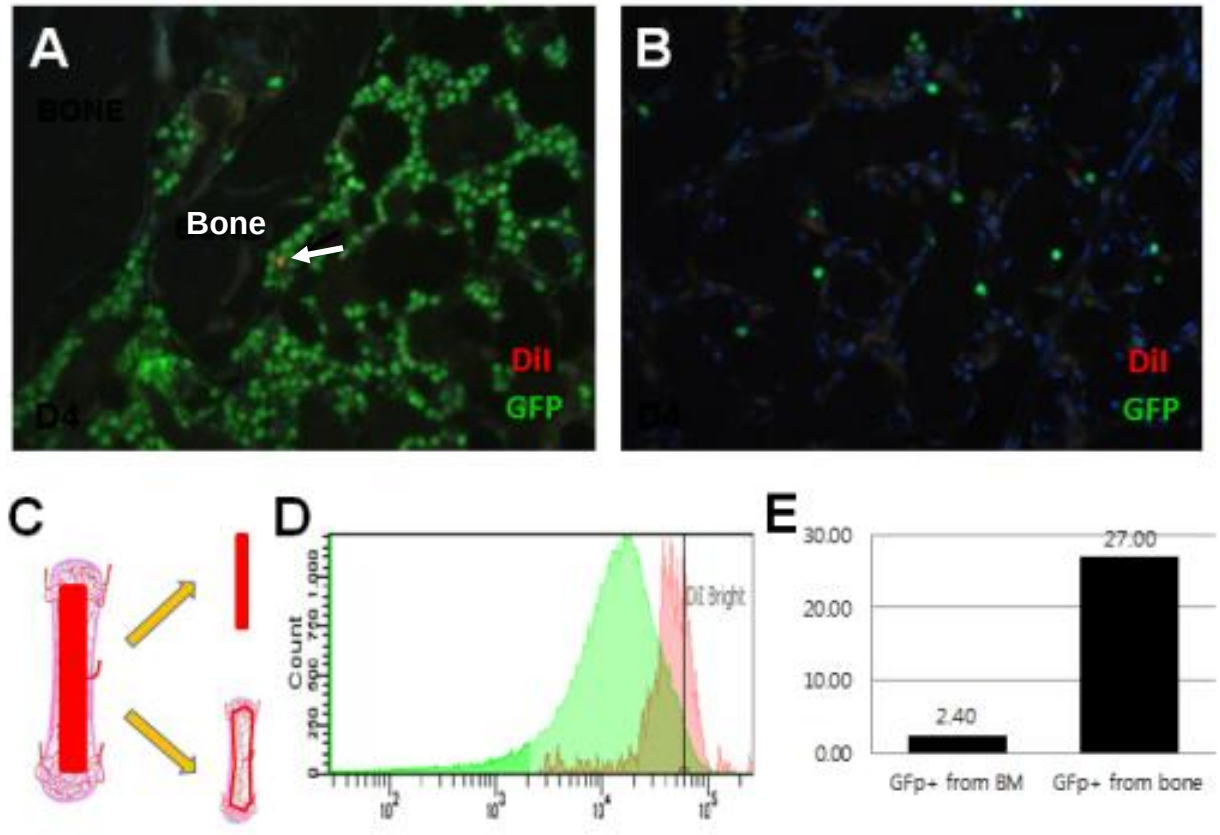

Figure 4-3. Histology and FACS analysis of the DiI dye stained GFP positive SKL cells. [A] DiI dye retaining cells can be observed on the endosteal surface (arrow). [B] Cells engrafted on the central marrow region did not retain DiI dye. [C] Experimental scheme to separate bone marrow mononuclear cells from the central marrow regions and endosteal regions. The detailed method was described in section 2. [D,E] FACS analysis shows that the endosteal region had significantly higher DiI bright cells.

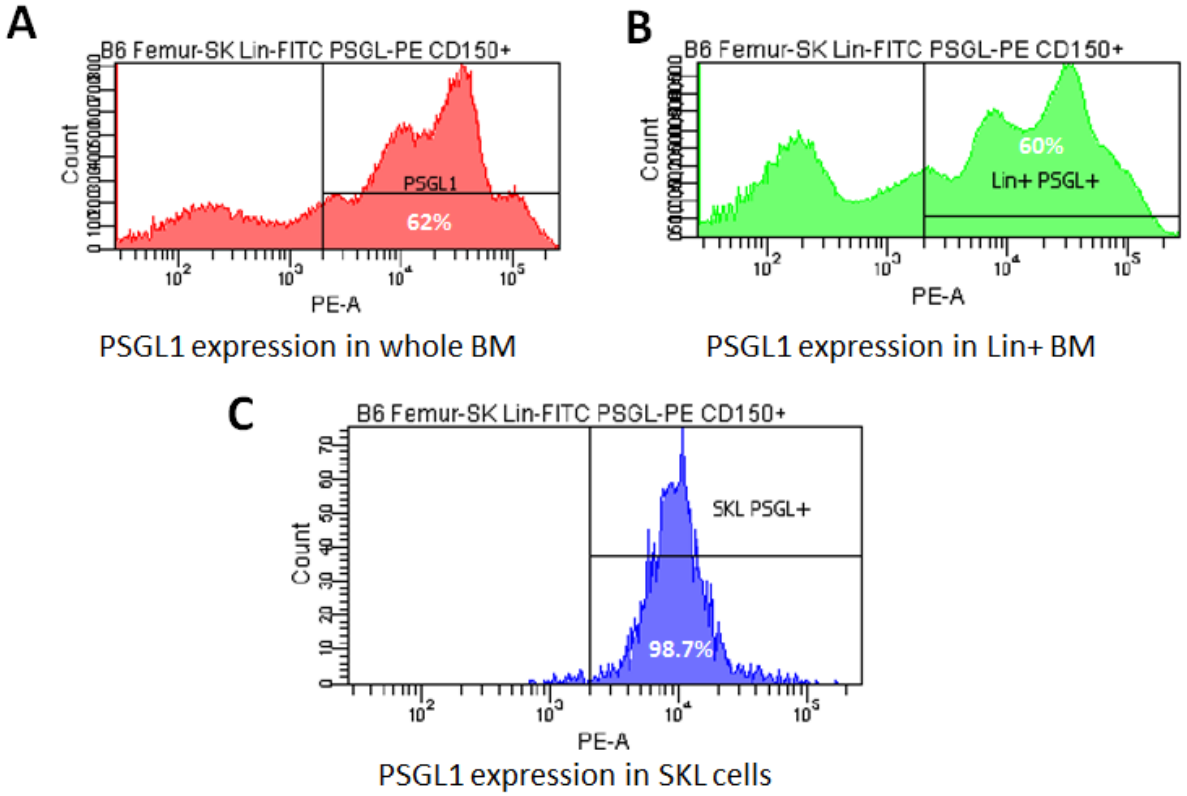

Figure 4-4. P-selectin ligand PSGL-1 expression in the bone marrow cells. [A] PSGL-1 gating for the whole bone marrow cells. [B] PSGL-1 gating for the lineage marker positive differentiated cells. [C] PSGL-1 gating of the SKL HSC. 98.7% of the SKL cells were PSGL-1 positive.

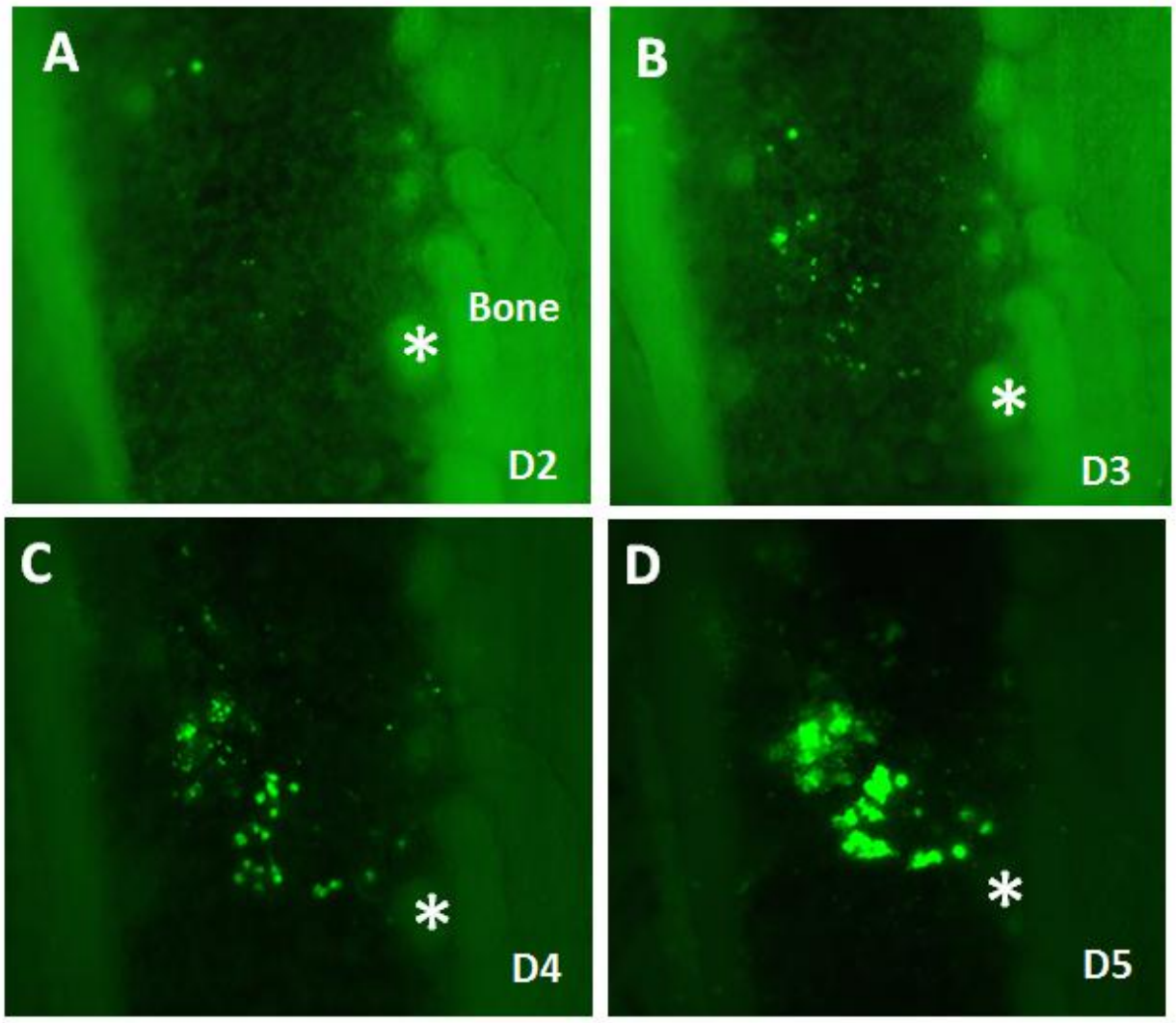

Figure 4-5. Engraftment pattern of the SKL HSC in the P-selectin knockout mice. [A] 48h after SKL HSC injection. HSCs were engrafted in the vascular niche. [B-D] Cells engrafted on the vascular niche continue to proliferate without migrating toward the osteoblastic niche. Asterisks are to mark the same location.

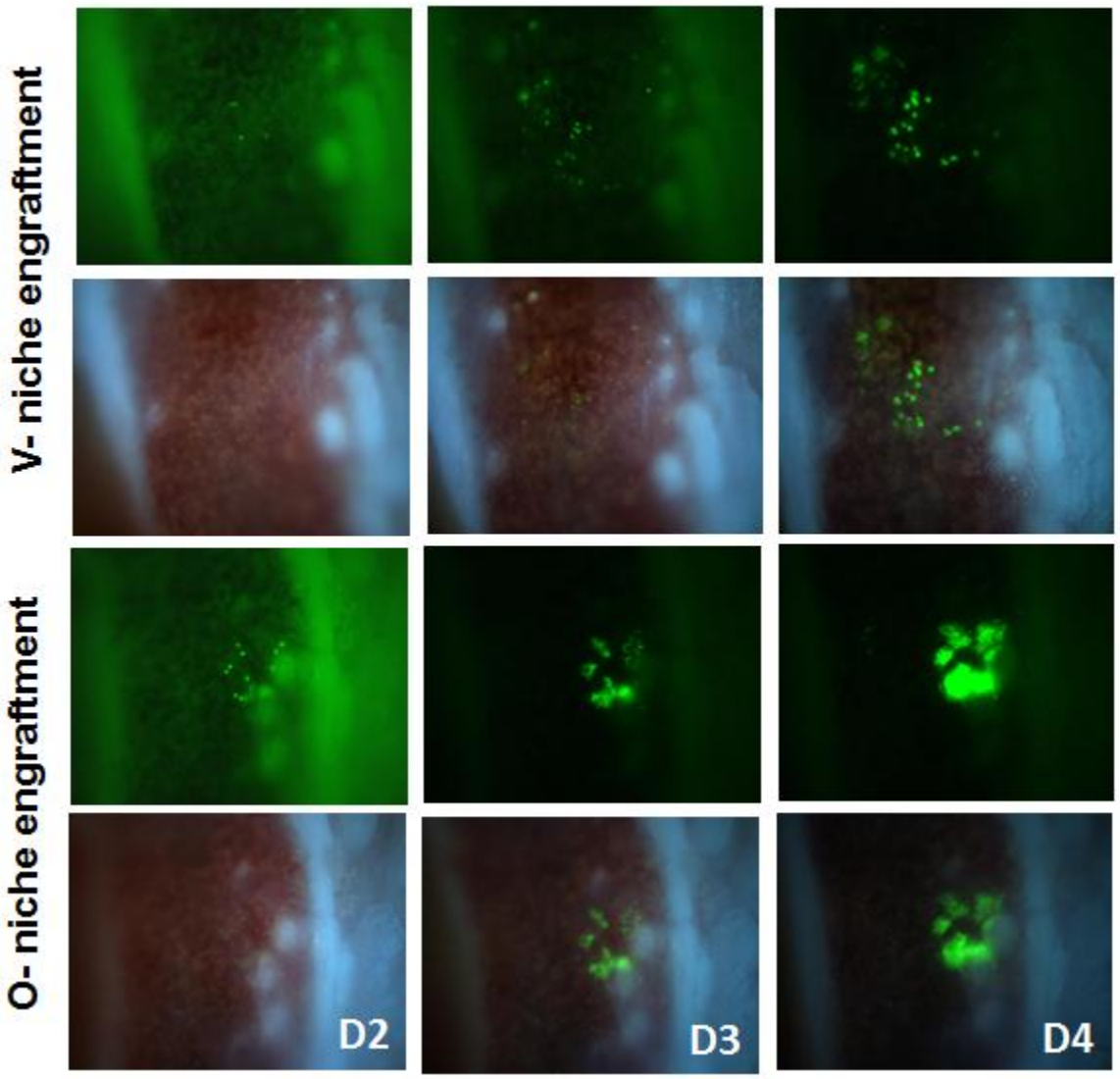

Figure 4-6. Different engraftment kinetics in the P-selectin knockout mice. Cells engrafted in the perivascular niche (v-niche) engraft and repopulate slower compared to the cells engrafted in the osteoblastic niche (o-niche).

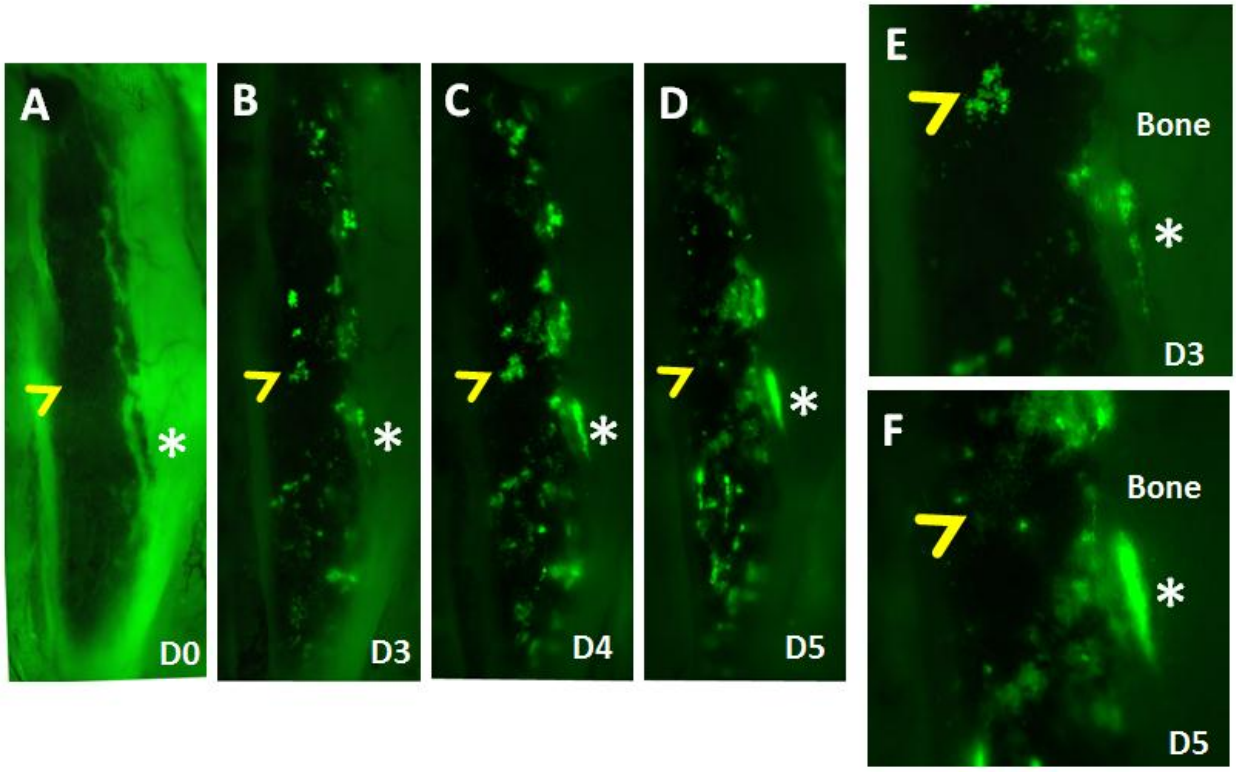

Figure 4-7. In vivo imaging of the tibia window in a representative osteopontin knockout mouse. [A-D] Low magnification mosaic images to display engraftment process in the whole tibia region. Arrows are to mark the same area and to indicate a developing colony originated from the vascular niche. [E-F] Higher magnification of the yellow arrowhead area showing failure of engraftment and proliferation in the vascular niche. Asterisks are to mark the same location and to indicate HSC engraftment in the osteoblastic niche.

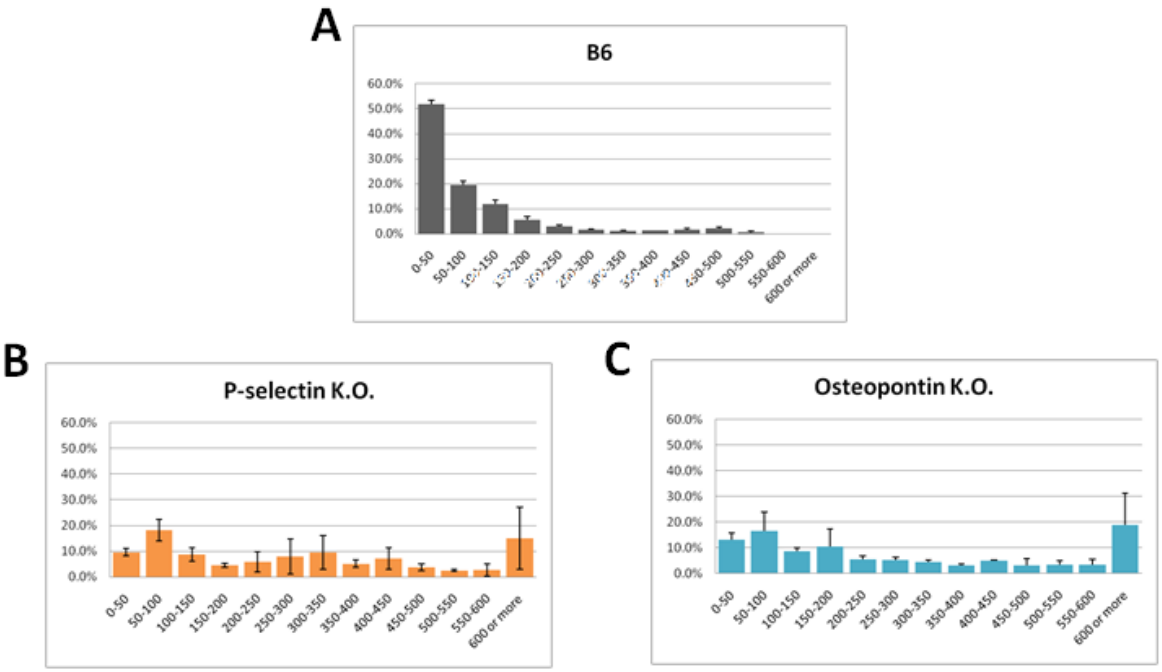

Figure 4-8. Measurement of the distance between the bone inner surface and the SKL HSCs 18h after cell injection.

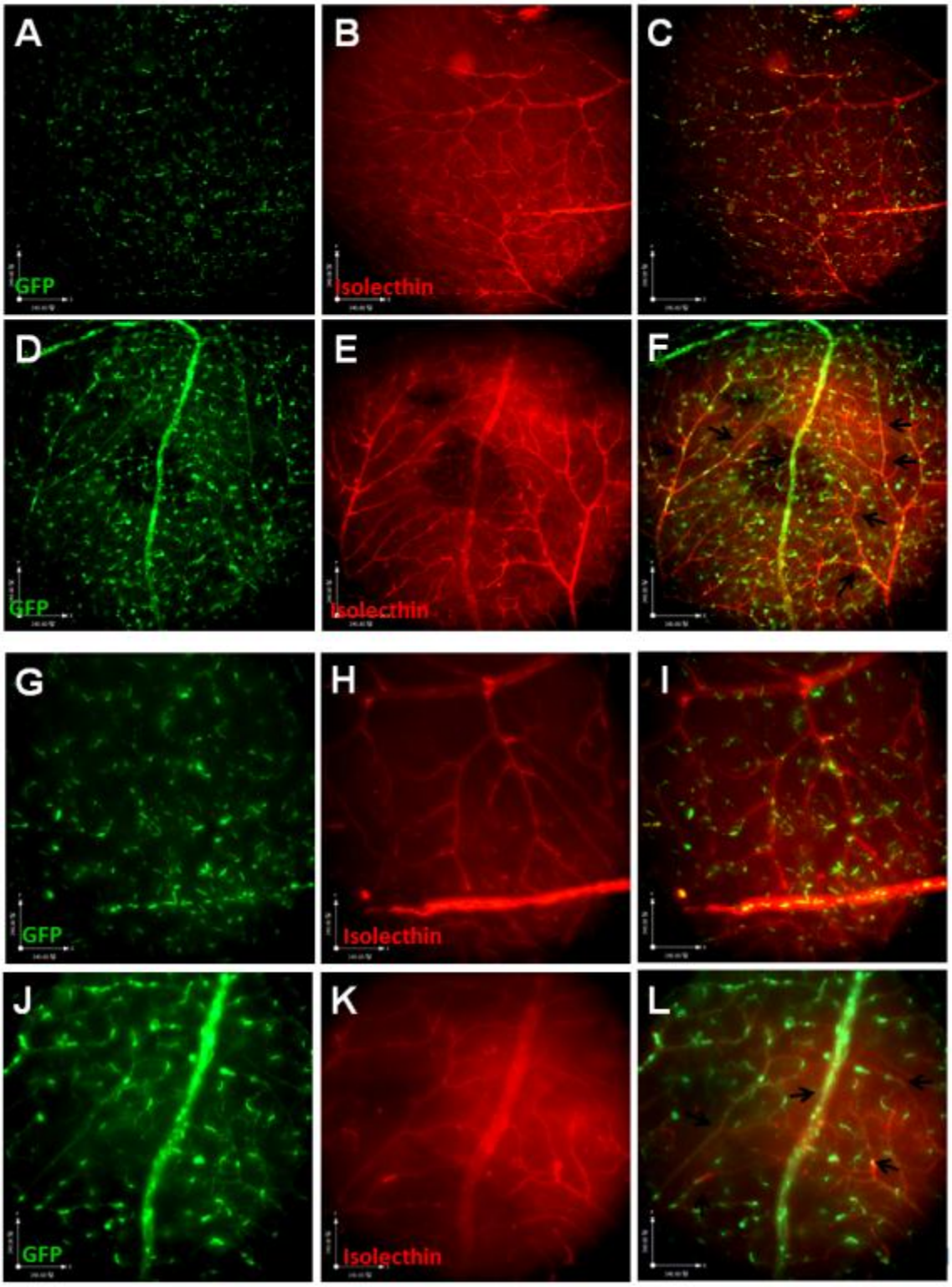

Figure 4-9. Whole mount of eyes from C57BL/6 (A-C, G-I) and osteopontin knockout mice (D-F, J-l) with laser injury to the eye after GFP BM transplantation. The eyes were stained with isolectin to visualize vessels.

CHAPTER 5
UNDERSTANDING THE HSC ENGRAFTMENT PROCESS

Introduction

Why do we need to know the relationships among hematopoietic stem cells (HSC) and cell types surrounding them in bone marrow? The general issue is whether the surrounding cells really matter in order to maintain HSC self-renewal ability. As discussed in Chapter 6, one of the important reasons why controversies began is that different research groups used different set of markers for HSC, different purification techniques, different bones (calvarial bones vs. long bones) and different animal models. To solve this problem, the traditional HSC cells (SKL, stem and progenitor cell mix) and LT-HSC (SLAM-SKL, more defined stem cell) that was first coined by Morrison et al. were directly compared in the tibia window (72). In addition, from the inconsistency of the BM and the peripheral blood result, I decided to investigate the spleen, the major extramedullary hematopoiesis organ. There are many indications that the spleen can play an important role in hematopoiesis, but it remains largely unstudied. We have known that hematopoietic stem cells (HSC) are trafficking during embryonic development through the spleen and reside withing the organ in postnatal hematopoiesis. By looking at the two different stem cell populations and the two major organs for hematopoiesis after irradiation, I aimed to present in depth analysis of the HSC engraftment process.

Engraftment Pattern of SLAM-SKL and SKL Cells

The next question was whether the observation that we had from the tibia window was cell specific. A recent paper suggests that SKL cells can further purified using the SLAM markers (CD48, CD150). When SKL cells were sorted based on CD150 positive

and negative for CD48, most of the stem cells were in the vascular niche (Figure 5-1). This suggested that it is not microenvironment but the type of the stem cell that determine its own microenvironment. However, considering that the SLAM-SKL population was derived from the SKL cells, I needed to understand more about the characteristics of each population. To further highlight the difference in engraftment pattern between SLAM-SKL cells and SKL cells and understand cell dynamics, the same number of each cell population from different mice (DsRed and GFP respectively) was sorted and injected into the C57B6 mice (Figure 5-2). As expected, SKL cells were engrafted mainly in the osteoblastic niche, but the SLAM-SKL cells were found mostly in the perivascular niche. This result is consistent with previous publications and suggests that SLAM-SKL cells use different mechanism for engraftment. In addition, although the same number of the each population was injected, SKL cells were 2-3.5 times more frequently observed in the tibia window within the very first 52 hours from cell injection (Figure 5-3). More interestingly, the ratio of the SLAM-SKL and SKL cells in the bone marrow and the peripheral blood was not consistent, but opposite of each other till the first week (Figure 5-4).

Engraftment, the First Week and Beyond

The result from Figure 5-4 suggested a possibility that either SLAM-SKL cells can differentiate into blood much quicker, or hematopoiesis occurred in extramedullary tissues such as spleen or liver. Indeed, the spleen had more SLAM-SKL derived cells at D14 (Fig. 5-5). This could be due to the different microenvironment in the spleen that has abundant blood vessel but no osteoblasts. Data from Figure 5-6 also demonstrated that the major cell population in the spleen and BM is different to each other. From the analysis of the peripheral blood, it is possible that the major organ that produces blood

in the early engraftment stage (between 7-14 days) is spleen and the explosive increase of the SLAM-SKL cells in the BM at the second week could be due to homing of the spleen originated SLAM-SKL cells back to BM.

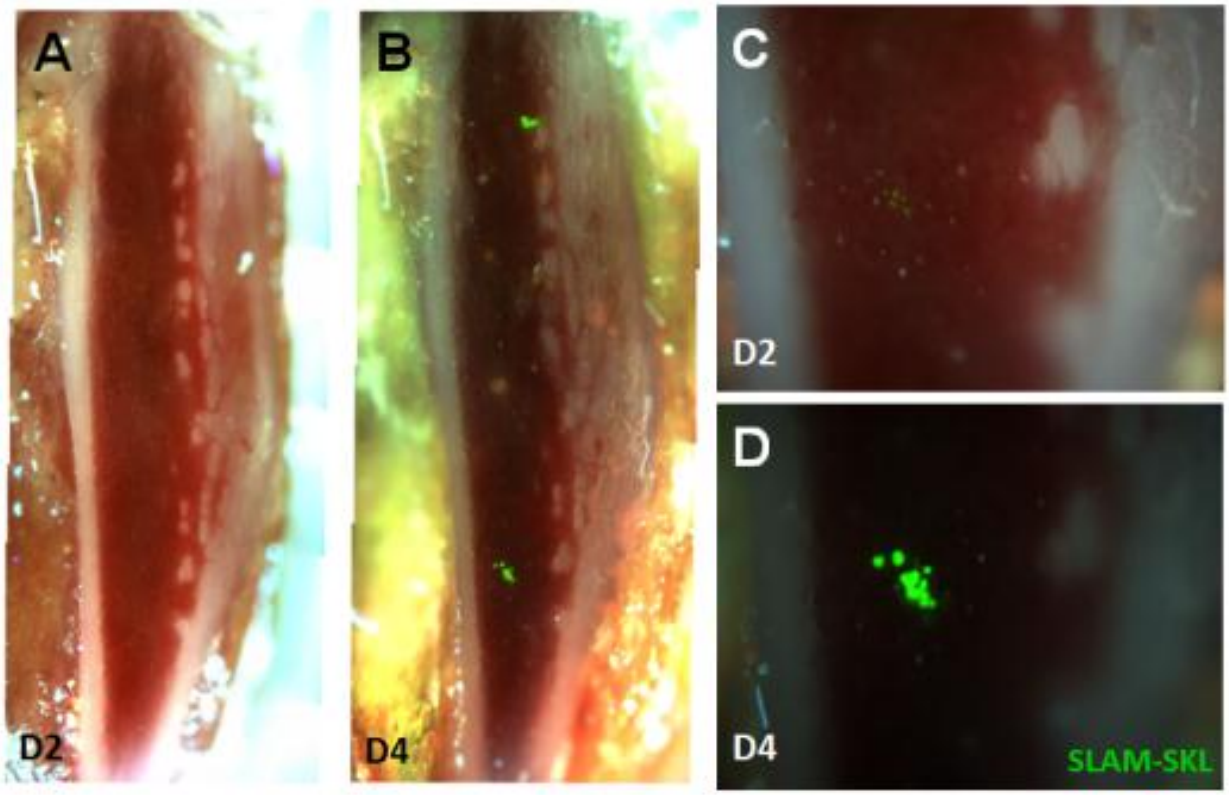

Figure 5-1. In vivo imaging of the tibia window in a C57BL6 mouse transplanted with $5X10^3$ CD150+ CD48- SKL (SLAM-SKL) cells. [A-B] Mosaic image of the tibia window at day 2 and day 4. Note the engraftment was limited to the central marrow region (the perivascular niche). [C-D] Higher magnification of the engrafted cells on the bottom.

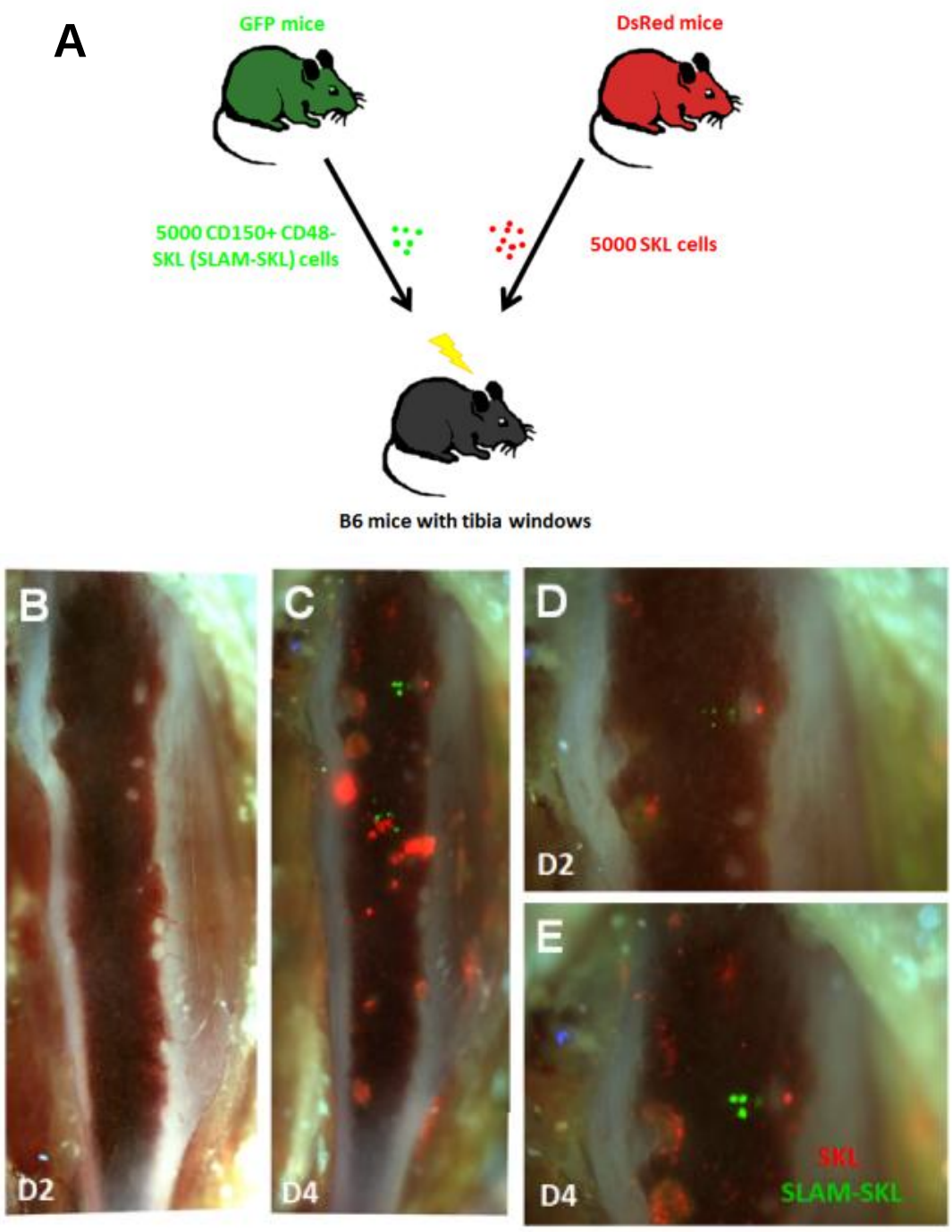

Figure 5-2. Competitive repopulation assay with the DsRed positive SKL cells and GFP positive SLAM-SKL cells. [A] Experimental scheme. [B-E] The mosaic image of the tibia window and the higher magnification of the animal.

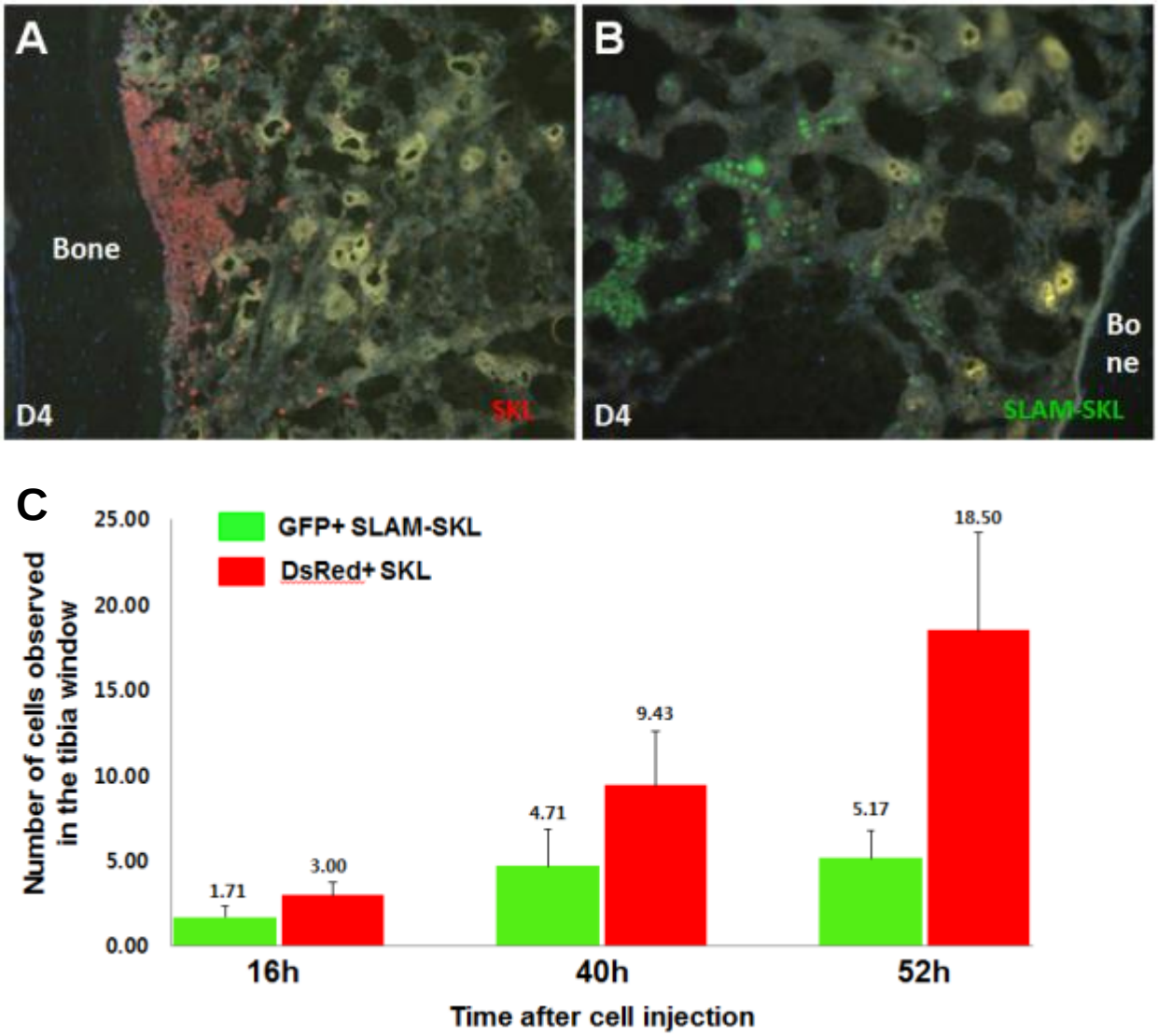

Figure 5-3. Engraftment pattern of the SKL cells and SLAM-SKL cells. [A] DsRed positive SKL cells were observed mainly on the endosteal region. [B] Most of the GFP positive SLAM-SKL cells were found on the central marrow region. [C] Average number of cells observed on the tibia window after the co-injection two different stem cells.

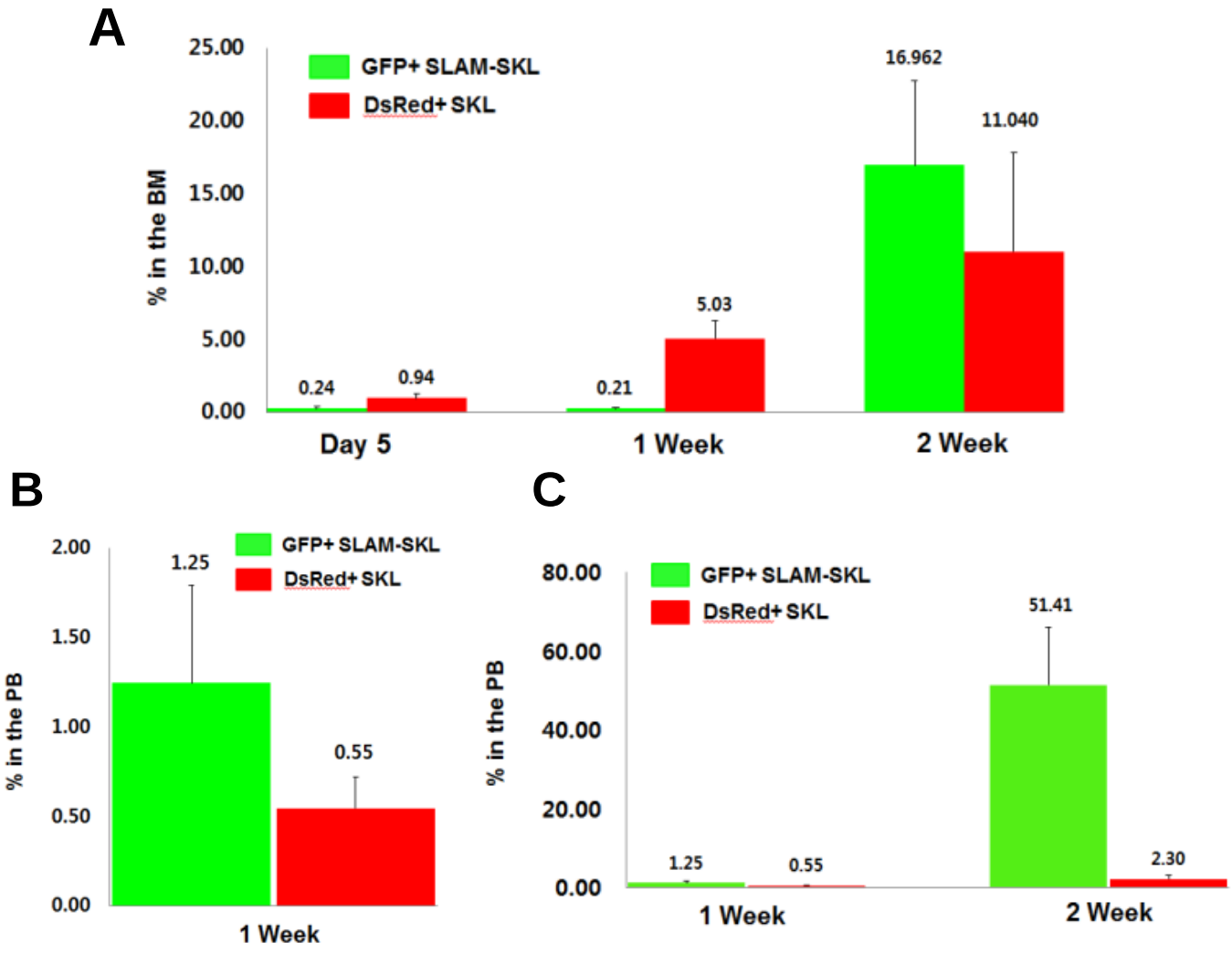

Figure 5-4. FACS analysis of the bone marrow and peripheral blood mononuclear cells. [A] Bone marrow analysis at day 5, 1 week and 2 week after cell injection. SKL cells prevail in the BM until the first week, but the number of SLAM-SKL cells was dramatically increased at the second week. [B] Peripheral blood cells originated from SLAM-SKL cells were more than twice compared to the cells from SKL cells at week 1. [C] The difference becomes even greater at 2 week which suggests that SLAM-SKL cells have better ability to generate blood.

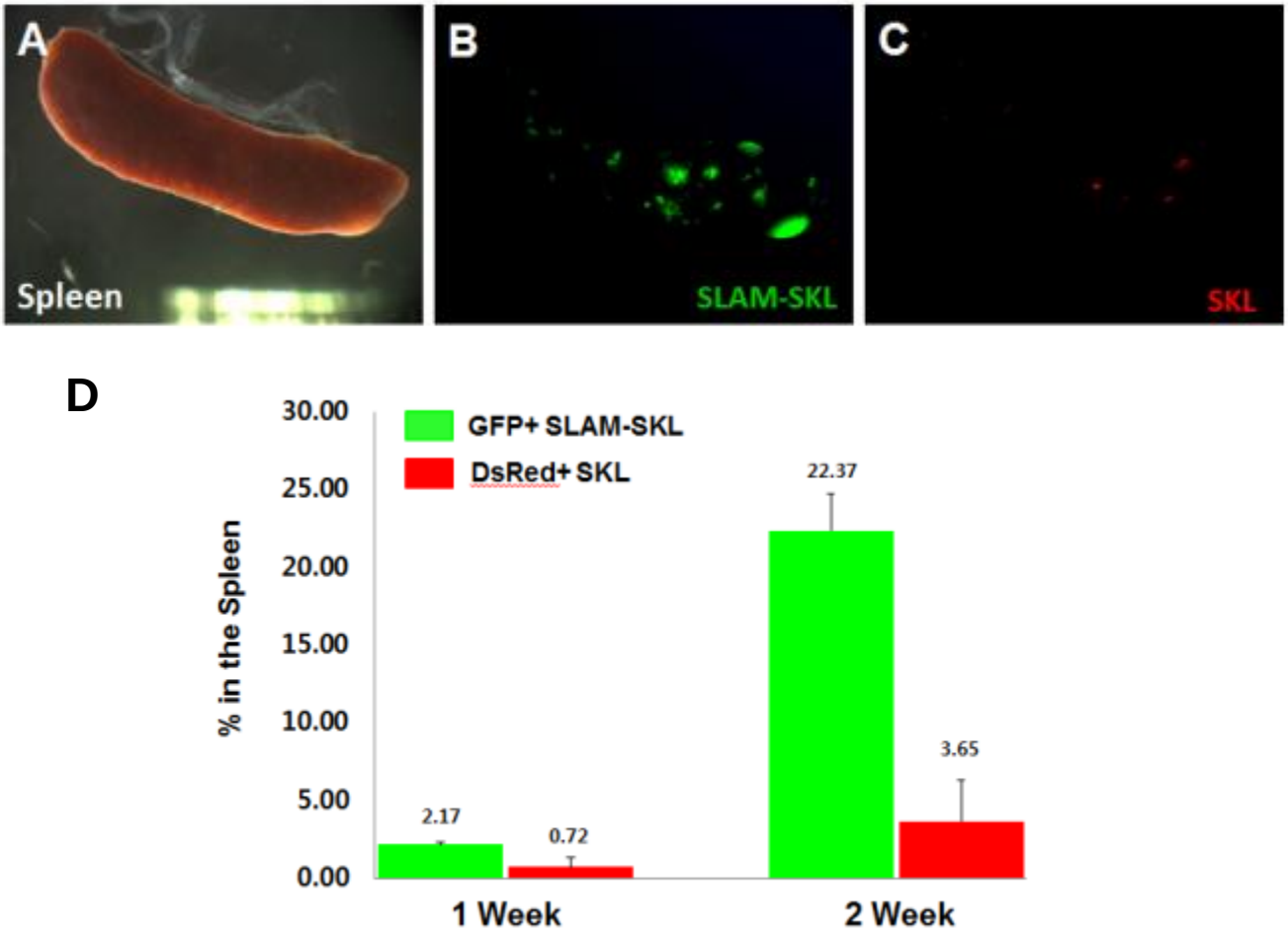

Figure 5-5. Analysis of the spleen to understand what cells engrafted in spleen microenvironment. [A-C] Direct visualization of the spleen transplanted with same numbers of SKL and SLAM-SKL cells. [D] FACS analysis of the each population in spleen at 1 and 2 week after cell injection.

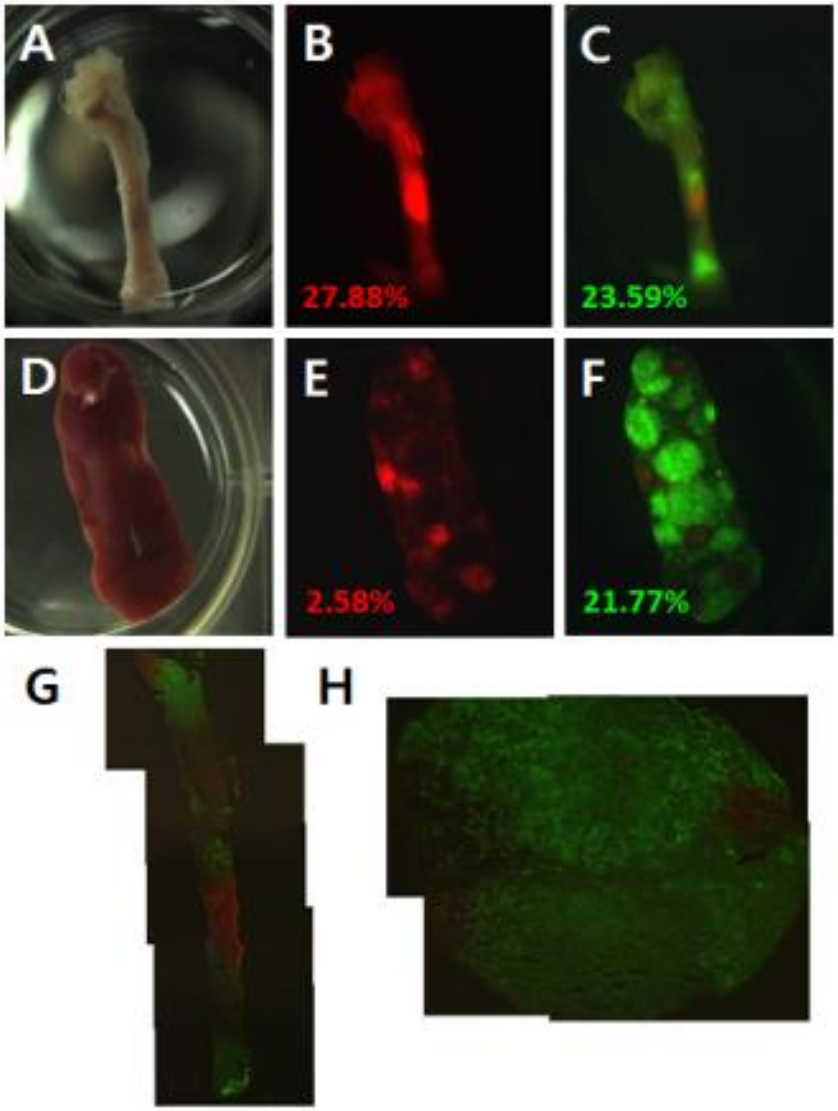

Figure 5-6. Comparison of the femur and spleen of a mouse transplanted with the same number of the SKL and SLAM-SKL cells. [A-C and D-F] The femur and spleen were directly visualized under a dissection scope. [G-H] Mosaic images of the sectioned femur and spleen in the OCT blocks.

CHAPTER 6
DISCUSSION

Stem cells are thought to reside in a special microenvironment called niche which supports their maintenance and regulates their function. Understanding stem cell niche is critical if we are to use stem cells to repair or restore damaged organs. Although the hematopoietic stem cell is well characterized, it is still unclear how the transplanted hematopoietic stem cells get engrafted in the bone microenvironment. There are few in vivo imaging techniques available to study the hematopoietic stem cell engraftment process after lethal irradiation. Therefore, my long term research goal was to develop an effective in vivo imaging technique for identifying where injected HSCs first engraft, how they re-populate within the stem cell niche, and what factors control these processes. The central hypothesis was that different stem cell populations have different homing and proliferation ability. The hypothesis was tested by addressing three specific aims. 1) I first determined whether HSC engraftment process can be visualized in real-time using invasive imaging technique (tibia window), validated the method by showing that only HSC can repopulate in the tibia window and confirmed what I observed from the tibia window using non-invasive magnetic resonance imaging technique. 2) I used cell tracking dyes and knockout mice to understand the difference between cells engrafted on the endosteal and perivascular niche in the tibia window model. The working hypothesis was that HSC from Sca-1+, c-Kit+ and lineage markers – population prefer to engraft into the osteoblastic niche, a hypothesis that is strongly supported by data shown here. 3) I aimed to understaned the HSC engraftment process in a broader view, by using two different stem cell populations (SKL and SLAM-SKL cells) and by analyzing not only bone marrow, but also peripheral blood and spleen. The

data shown here clearly suggest that each stem cell population based on different markers lodges in different niche and the spleen can play a critical role during the initial phase of the engraftment (Fig. 6-1). This finding is important to consider in several clinical approaches such as the bone marrow transplantation and the leukemia therapy.

Homing and lodgment of HSCs in the appropriate microenvironmental niche are the two essential steps that are directly related to the clinical outcome of BM transplantation (18). Following BM transplantation, HSC cells are guided by the stromal cells for migration process. At the destination, the niche cells provide important signaling cues for the HSCs to undergo either self-renewal or controlled proliferation for the repopulation of the hematopoietic cells in the recipient. Although many studies have demonstrated that various factors that are involved in regulating the capability of transplanted HSCs to engraft, the precise cellular and molecular mechanisms that drive the transplanted HSCs to undergo trans-marrow migration and localization and anchoring in a specific niche are still unclear. The data presented here demonstrated that the self-renewal and proliferation of the HSC occurred mainly in the osteoblastic niche. This suggests that expansion of the osteoblast population in the BM can facilitate the HSC engraftment (18, 34, 41, 43). Identifying the adhesion molecules and other regulating factors that are present in the microenvironment are of great interest in the stem cell field and are still currently under investigation. If we can understand the underlying mechanisms that promote the engraftment and regeneration of hematopoiesis in a myelo-ablative recipient, it would be vastly beneficial in advancing the current approaches for treating and preventing malignant blood disorders, especially in the clinical transplantation setting.

The analysis of stem cell–niche interactions in the Drosophila germ line clearly demonstrated that one niche cell type support a single stem cell (69). However, this model appears unlikely to be conserved in the hematopoietic system, simply because the microenvironment of the bone has too many players that affect HSC quiescence, proliferation and differentiation. An important consideration in determining the HSC niche is how we define the microenvironment. Is it the location of the engrafted and lodged HSC in the bone marrow after the lethal irradiation? In such a scenario, how one can predict that the cells that were found either in the osteoblastic niche or in the perivascular niche have the true stem cell potentials such as self-renewal, proliferation and differentiation? Histology analysis reveal information on only one time point and a single cell in the osteoblastic or perivascular niche does not mean that the cell reached its final destination and would undergo stem cell activity at the site. In addition, studies localizing the donor derived HSCs at early time points after lethal irradiation may also not reveal the true niche in the normal physiological state, as the bone marrow microenvironment is rapidly and dramatically changed by the irradiation procedure (70, 71). Then an even more difficult question would be what kind of HSC we should use to determine the HSC niche as there are dozens of methods to purify HSCs and they are all different to each other (59). There should be more stringent criteria to define the HSC niche, such as defining the microenvironment that functionally supports lodgment, proliferation and quiescence of the transplanted stem cell. It has been difficult to observe this niche so far because of the lack of in vivo imaging methods. Using the time-lapse in vivo imaging on the tibia window made it possible to monitor the

transplanted HSC to engraft, proliferate or become quiescent in both irradiation and non-irradiation model as shown in this dissertation.

The fact that DiI retained HSC cells were found only near the endosteal region warrants further investigation. What would be the mechanisms to make the endosteum bound cells quiescent while the surrounding HSC rapidly expand? Is there any specific type of the bone lining cells that has this ability? There have been many reports suggesting that the HSC niche is located within the osteoblastic niche (33, 36-42). This area includes not only the direct borders between the bone and BM but also trabecular regions made up with spicules, and also the region within 8-10 cell distance from the endosteum (17, 19, 36, 72). At this location, HSPC reside on the endosteal surface having direct binding with osteoblasts, having adhesive interaction with the extracellular components of the bone. Another possibility is that the HSPC locate in very close proximity to bone and affected by the factors secreted directly from the bone lining cells such as osteoblasts or osteoclasts (41, 43). The data presented here also highlight that the purified SKL HSC prefer to locate near the endosteum and further start to proliferate by forming colonies along the bone area. While expansion of the osteoblast is clearly related to the increase of HSC in the microenvironment, suppression of the osteoblast in mice has not consistently shown the reduction of the HSC number in the BM. Visnjic et al. demonstrated conditional deletion of the osteoblasts by gancyclovir resulted in reduction of the HSC number and extrameduallary hematopoiesis in the liver and the spleen (42), but Kiel et al. demonstrated that osteoblast dysfunction in the biglycan deficient mouse did not trigger any changes in HSC number and activity in the BM (73, 74). In the experiment using the p-selectin knockout mice, I demonstrated that the

injected SKL cells also could proliferate in the perivascular niche although it was less efficient to the cells engrafted in the osteoblastic niche, and this suggests that the SKL cells can survive and proliferate in the central marrow region when it has no other choice. Therefore, the interaction between osteoblast and the SKL cells can be dispensable, but necessary for efficient HSC engraftment and proliferation.

Whether the direct cell to cell interaction with the osteoblasts is absolutely critical or not is unclear, but the ex vivo high magnification image suggests that the SKL cell bound on the inner bone surface can form a tight junction with the osteoblast in the very early engraftment stage before they proliferate. This, in turn, emphasizes the use of a correct method to collect BM mononuclear cells as it may be critical to collect the BM cells directly bound to the bone. As flushing the bone marrow with a syringe cannot elute such population, it may be ideal to grind the bone in the mortar with the pestle after flushing, and further extract cells that are attached to the endosteal surface by treating enzymes such as collagenease I and dispase to collect BM mononuclear cells with bone interactions. The number of stem cells, the potency of the stem cells can be different depending on what method is used for cell collection and this may partly explain inconsistencies among publications on the HSC niche.

As the different cell collection methods among publications do not fully explicate the different engraftment pattern between SKL and SLAM-SKL populations in the tibia window model, the results from the competitive repopulation assay in GFP+ SLAM-SKL cells and DsRed+ SKL cell need further attention. It is very interesting that the subpopulation of the SKL cells, CD150+ and CD48- SKL cells can engraft different microenvironment compared to SKL population. It should be noted that the SKL cells

are about 0.5% of the whole BM cells and SLAM-SKL cells are around 0.002%. As only one in 250 SKL cells is the SLAM-SKL cells, it is possible that the subpopulation have its own characteristics for engraftment and proliferation. Since the majority of the BM cells are negative for other SLAM family markers such as CD48 or CD41, the critical determination factor for SLAM-SKL cells should be CD150, which is expressed in less than 1% of the BM cells. It is arguable whether CD150 negative cells also have a long term repopulation capacity (75), but several papers suggest that CD150 is the key marker for LT-HSC (49, 76, 77). As the vascular niche is thought to be a dynamic scaffold that supports both stem precursor cells and is ideal for rapid hematopoietic cell production, the SLAM-SKL cells in the vascular niche will actively generate blood cells release them into circulation. Indeed, more than 70% of SLAM-SKL HSCs express CD34 (8), a marker that is normally associated with activated or short-term repopulating HSCs (78, 79). In addition, the majority of HSCs identified using SLAM markers are not BrdU label-retaining cells (76). Therefore, the SLAM-SKL population may not be the true LT-HSC, but a subpopulation of SKL cells with different cell dynamics. CD150+ CD48- SKL cells have an alternative HSC niche in mice with lethal irradiation and this was clearly demonstrated in data presented here. The next logical question is, whether the LT-HSC, defined as CD150+, CD48- SKL cells are located in the vascular niche of the bone marrow during the normal physiological state. As we come to know more about the HSC engraftment process, it becomes even more complex than originally thought and further studies are required to better understand the early stage of the engraftment process.

The ability of HSC to exist not only to the bone marrow but also to spleen was demonstrated decades ago in an experiment that shielding of the spleen with lead during the lethal irradiation allowed mice to survive (80). The other studies in the following decade (81, 82) clearly demonstrated that HSC exist in spleen could spontaneously “home” to and repopulate the bone marrow (21, 83). The finding that the transplanted SLAM-SKL cells were mostly found in the spleen during the extramedullary hematopoiesis in the first week of the engraftment suggests that the spleen plays a critical role in the initial stage of the engraftment. Since the spleen has no osteoblatic lineage cells, it is possible the SLAM-SKL cells, which were found mainly in the perivascular niche in the bone marrow, favored to be engrafted in the spleen microenvironment. The explosive increase of the SLAM-SKL cells in the BM at two week and the circulating SLAM-SKL cells in the live imaging make us hypothesize that the SLAM-SKL cells in the spleen mobilize toward the BM after the microenvironment of the BM recovers from irradiation. This is the reason that we should understand the HSC engraftment process in a broader view as the results presented here imply that the event occurs in several microenvironments in the system and they can affect each other during the engraftment process.

HSC engraftment is a very dynamic and complex process and many stem cell niches are involved during the process (Figure 6-1). Bone marrow transplantation is routinely done to correct various hematopoietic malignancies. By using the novel in vivo imaging techniques described here, we will be able to understand how the transplanted HSCs get engrafted in the bone microenvironment and this will greatly impact treatment strategies of hematopoietic diseases.

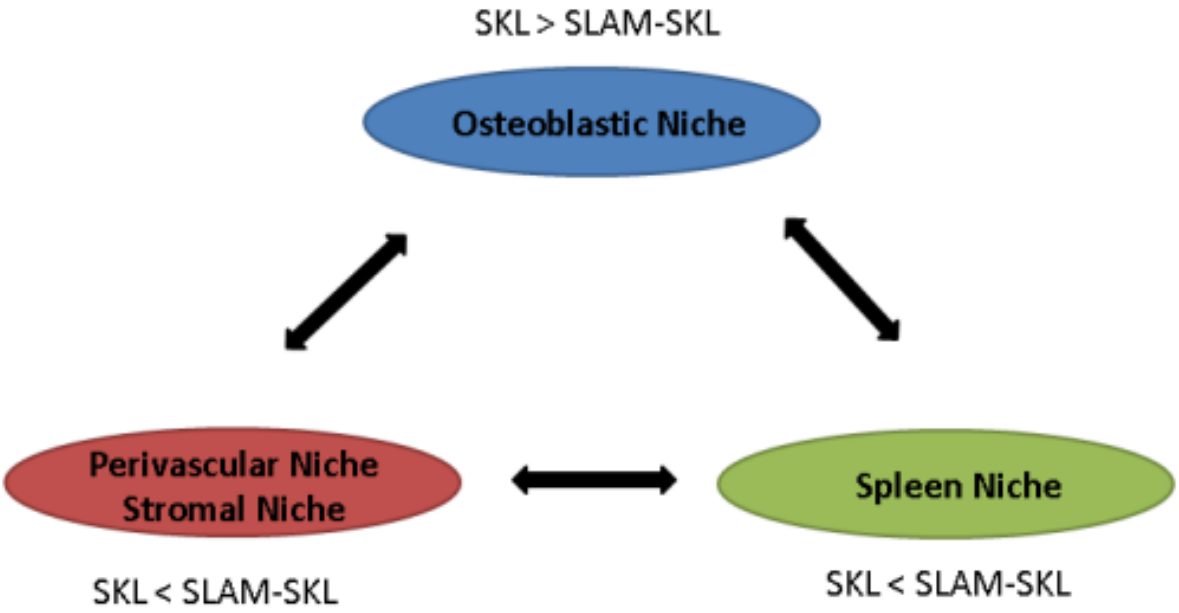

Figure 6-1. A schematic diagram that suggests interactions of the three important HSC niches.

LIST OF REFERENCES

1. Thomas, E.D., Lochte, H.L., Jr., Lu, W.C., and Ferrebee, J.W. 1957. Intravenous infusion of bone marrow in patients receiving radiation and chemotherapy. *N Engl J Med* 257:491-496.

2. Lord, B.I., and Hendry, J.H. 1972. The distribution of haemopoietic colony-forming units in the mouse femur, and its modification by x rays. *Br J Radiol* 45:110-115.

3. Lord, B.I., Testa, N.G., and Hendry, J.H. 1975. The relative spatial distributions of CFUs and CFUc in the normal mouse femur. *Blood* 46:65-72.

4. Mason, T.M., Lord, B.I., and Hendry, J.H. 1989. The development of spatial distributions of CFU-S and in-vitro CFC in femora of mice of different ages. *Br J Haematol* 73:455-461.

5. Lambertsen, R.H., and Weiss, L. 1984. A model of intramedullary hematopoietic microenvironments based on stereologic study of the distribution of endocloned marrow colonies. *Blood* 63:287-297.

6. Schofield, R. 1978. The relationship between the spleen colony-forming cell and the haemopoietic stem cell. *Blood Cells* 4:7-25.

7. Schofield, R., and Lajtha, L.G. 1983. Determination of the probability of self-renewal in haemopoietic stem cells: a puzzle. *Blood Cells* 9:467-483.

8. Wilson, A., Oser, G.M., Jaworski, M., Blanco-Bose, W.E., Laurenti, E., Adolphe, C., Essers, M.A., Macdonald, H.R., and Trumpp, A. 2007. Dormant and self-renewing hematopoietic stem cells and their niches. *Ann N Y Acad Sci* 1106:64-75.

9. Wilson, A., and Trumpp, A. 2006. Bone-marrow haematopoietic-stem-cell niches. *Nat Rev Immunol* 6:93-106.

10. Slezak, S.E., and Muirhead, K.A. 1991. Radioactive cell membrane labelling. *Nature* 352:261-262.

11. Spangrude, G.J., Brooks, D.M., and Tumas, D.B. 1995. Long-term repopulation of irradiated mice with limiting numbers of purified hematopoietic stem cells: in vivo expansion of stem cell phenotype but not function. *Blood* 85:1006-1016.

12. Hendrikx, P.J., Vermeulen, J., Hagenbeek, A., Vermey, M., and Martens, A.C. 1996. LacZ staining in paraffin-embedded tissue sections. *J Histochem Cytochem* 44:1323-1329.

13. Nilsson, S.K., Dooner, M.S., Tiarks, C.Y., Weier, H.U., and Quesenberry, P.J. 1997. Potential and distribution of transplanted hematopoietic stem cells in a nonablated mouse model. *Blood* 89:4013-4020.

14. Nilsson, S.K., Hulspas, R., Weier, H.U., and Quesenberry, P.J. 1996. In situ detection of individual transplanted bone marrow cells using FISH on sections of paraffin-embedded whole murine femurs. *J Histochem Cytochem* 44:1069-1074.

15. Lanzkron, S.M., Collector, M.I., and Sharkis, S.J. 1999. Hematopoietic stem cell tracking in vivo: a comparison of short-term and long-term repopulating cells. *Blood* 93:1916-1921.

16. Parish, C.R. 1999. Fluorescent dyes for lymphocyte migration and proliferation studies. *Immunol Cell Biol* 77:499-508.

17. Nilsson, S.K., Johnston, H.M., and Coverdale, J.A. 2001. Spatial localization of transplanted hemopoietic stem cells: inferences for the localization of stem cell niches. *Blood* 97:2293-2299.

18. Lam, B.S., and Adams, G.B. Hematopoietic stem cell lodgment in the adult bone marrow stem cell niche. *Int J Lab Hematol* 32:551-558.

19. Nilsson, S.K., Simmons, P.J., and Bertoncello, I. 2006. Hemopoietic stem cell engraftment. *Exp Hematol* 34:123-129.

20. Mazo, I.B., Gutierrez-Ramos, J.C., Frenette, P.S., Hynes, R.O., Wagner, D.D., and von Andrian, U.H. 1998. Hematopoietic progenitor cell rolling in bone marrow microvessels: parallel contributions by endothelial selectins and vascular cell adhesion molecule 1. *J Exp Med* 188:465-474.

21. Magnon, C., and Frenette, P.S. 2008. Hematopoietic stem cell trafficking.

22. Katayama, Y., Hidalgo, A., Furie, B.C., Vestweber, D., Furie, B., and Frenette, P.S. 2003. PSGL-1 participates in E-selectin-mediated progenitor homing to bone marrow: evidence for cooperation between E-selectin ligands and alpha4 integrin. *Blood* 102:2060-2067.

23. Ellis, S.L., Grassinger, J., Jones, A., Borg, J., Camenisch, T., Haylock, D., Bertoncello, I., and Nilsson, S.K. The relationship between bone, hemopoietic stem cells, and vasculature. *Blood* 118:1516-1524.

24. Nilsson, S.K., Johnston, H.M., Whitty, G.A., Williams, B., Webb, R.J., Denhardt, D.T., Bertoncello, I., Bendall, L.J., Simmons, P.J., and Haylock, D.N. 2005. Osteopontin, a key component of the hematopoietic stem cell niche and regulator of primitive hematopoietic progenitor cells. *Blood* 106:1232-1239.

25. Stier, S., Ko, Y., Forkert, R., Lutz, C., Neuhaus, T., Grunewald, E., Cheng, T., Dombkowski, D., Calvi, L.M., Rittling, S.R., et al. 2005. Osteopontin is a hematopoietic stem cell niche component that negatively regulates stem cell pool size. *J Exp Med* 201:1781-1791.

26. Denhardt, D.T., Giachelli, C.M., and Rittling, S.R. 2001. Role of osteopontin in cellular signaling and toxicant injury. *Annu Rev Pharmacol Toxicol* 41:723-749.

27. Rittling, S.R., and Denhardt, D.T. 1999. Osteopontin function in pathology: lessons from osteopontin-deficient mice. *Exp Nephrol* 7:103-113.

28. Denhardt, D.T. 2003. Commentary re: Q-T Le et al, identification of osteopontin as a prognostic marker for head and neck squamous cell carcinomas. clin cancer res, 9: 31-32, 2003. *Clin Cancer Res* 9:31-32.

29. McGrath, K.E., Koniski, A.D., Maltby, K.M., McGann, J.K., and Palis, J. 1999. Embryonic expression and function of the chemokine SDF-1 and its receptor, CXCR4. *Dev Biol* 213:442-456.

30. Nagasawa, T., Hirota, S., Tachibana, K., Takakura, N., Nishikawa, S., Kitamura, Y., Yoshida, N., Kikutani, H., and Kishimoto, T. 1996. Defects of B-cell lymphopoiesis and bone-marrow myelopoiesis in mice lacking the CXC chemokine PBSF/SDF-1. *Nature* 382:635-638.

31. Tachibana, K., Hirota, S., Iizasa, H., Yoshida, H., Kawabata, K., Kataoka, Y., Kitamura, Y., Matsushima, K., Yoshida, N., Nishikawa, S., et al. 1998. The chemokine receptor CXCR4 is essential for vascularization of the gastrointestinal tract. *Nature* 393:591-594.

32. Ma, Q., Jones, D., and Springer, T.A. 1999. The chemokine receptor CXCR4 is required for the retention of B lineage and granulocytic precursors within the bone marrow microenvironment. *Immunity* 10:463-471.

33. Glodek, A.M., Le, Y., Dykxhoorn, D.M., Park, S.Y., Mostoslavsky, G., Mulligan, R., Lieberman, J., Beggs, H.E., Honczarenko, M., and Silberstein, L.E. 2007. Focal adhesion kinase is required for CXCL12-induced chemotactic and pro-adhesive responses in hematopoietic precursor cells. *Leukemia* 21:1723-1732.

34. Calvi, L.M., Adams, G.B., Weibrecht, K.W., Weber, J.M., Olson, D.P., Knight, M.C., Martin, R.P., Schipani, E., Divieti, P., Bringhurst, F.R., et al. 2003. Osteoblastic cells regulate the haematopoietic stem cell niche. *Nature* 425:841-846.

35. Taichman, R.S. 2005. Blood and bone: two tissues whose fates are intertwined to create the hematopoietic stem-cell niche. *Blood* 105:2631-2639.

36. Yin, T., and Li, L. 2006. The stem cell niches in bone. *J Clin Invest* 116:1195-1201.

37. Martin, T.J., and Sims, N.A. 2005. Osteoclast-derived activity in the coupling of bone formation to resorption. *Trends Mol Med* 11:76-81.

38. Zhang, J., Niu, C., Ye, L., Huang, H., He, X., Tong, W.G., Ross, J., Haug, J., Johnson, T., Feng, J.Q., et al. 2003. Identification of the haematopoietic stem cell niche and control of the niche size. *Nature* 425:836-841.

39. Kinashi, T., and Springer, T.A. 1994. Steel factor and c-kit regulate cell-matrix adhesion. *Blood* 83:1033-1038.

40. Kovach, N.L., Lin, N., Yednock, T., Harlan, J.M., and Broudy, V.C. 1995. Stem cell factor modulates avidity of alpha 4 beta 1 and alpha 5 beta 1 integrins expressed on hematopoietic cell lines. *Blood* 85:159-167.

41. Adams, G.B., Martin, R.P., Alley, I.R., Chabner, K.T., Cohen, K.S., Calvi, L.M., Kronenberg, H.M., and Scadden, D.T. 2007. Therapeutic targeting of a stem cell niche. *Nat Biotechnol* 25:238-243.

42. Visnjic, D., Kalajzic, Z., Rowe, D.W., Katavic, V., Lorenzo, J., and Aguila, H.L. 2004. Hematopoiesis is severely altered in mice with an induced osteoblast deficiency. *Blood* 103:3258-3264.

43. Adams, G.B., Chabner, K.T., Alley, I.R., Olson, D.P., Szczepiorkowski, Z.M., Poznansky, M.C., Kos, C.H., Pollak, M.R., Brown, E.M., and Scadden, D.T. 2006. Stem cell engraftment at the endosteal niche is specified by the calcium-sensing receptor. *Nature* 439:599-603.

44. Taichman, R.S., and Emerson, S.G. 1998. The role of osteoblasts in the hematopoietic microenvironment. *Stem Cells* 16:7-15.

45. Taichman, R.S., and Emerson, S.G. 1994. Human osteoblasts support hematopoiesis through the production of granulocyte colony-stimulating factor. *J Exp Med* 179:1677-1682.

46. Taichman, R.S., Reilly, M.J., and Emerson, S.G. 2000. The Hematopoietic Microenvironment: Osteoblasts and The Hematopoietic Microenvironment. *Hematology* 4:421-426.

47. Winkler, I.G., and Levesque, J.P. 2006. Mechanisms of hematopoietic stem cell mobilization: when innate immunity assails the cells that make blood and bone. *Exp Hematol* 34:996-1009.

48. Sipkins, D.A., Wei, X., Wu, J.W., Runnels, J.M., Cote, D., Means, T.K., Luster, A.D., Scadden, D.T., and Lin, C.P. 2005. In vivo imaging of specialized bone marrow endothelial microdomains for tumour engraftment. *Nature* 435:969-973.

49. Kiel, M.J., Yilmaz, O.H., Iwashita, T., Yilmaz, O.H., Terhorst, C., and Morrison, S.J. 2005. SLAM family receptors distinguish hematopoietic stem and progenitor cells and reveal endothelial niches for stem cells. *Cell* 121:1109-1121.

50. Butler, J.M., Nolan, D.J., Vertes, E.L., Varnum-Finney, B., Kobayashi, H., Hooper, A.T., Seandel, M., Shido, K., White, I.A., Kobayashi, M., et al. Endothelial cells are essential for the self-renewal and repopulation of Notch-dependent hematopoietic stem cells. *Cell Stem Cell* 6:251-264.

51. Hooper, A.T., Butler, J.M., Nolan, D.J., Kranz, A., Iida, K., Kobayashi, M., Kopp, H.G., Shido, K., Petit, I., Yanger, K., et al. 2009. Engraftment and reconstitution of hematopoiesis is dependent on VEGFR2-mediated regeneration of sinusoidal endothelial cells. *Cell Stem Cell* 4:263-274.

52. Kopp, H.G., Avecilla, S.T., Hooper, A.T., and Rafii, S. 2005. The bone marrow vascular niche: home of HSC differentiation and mobilization. *Physiology (Bethesda)* 20:349-356.

53. Purton, L.E., and Scadden, D.T. 2008. The hematopoietic stem cell niche.

54. Mendez-Ferrer, S., Michurina, T.V., Ferraro, F., Mazloom, A.R., Macarthur, B.D., Lira, S.A., Scadden, D.T., Ma'ayan, A., Enikolopov, G.N., and Frenette, P.S. Mesenchymal and haematopoietic stem cells form a unique bone marrow niche. *Nature* 466:829-834.

55. Mendez-Ferrer, S., Chow, A., Merad, M., and Frenette, P.S. 2009. Circadian rhythms influence hematopoietic stem cells. *Curr Opin Hematol* 16:235-242.

56. Mendez-Ferrer, S., Lucas, D., Battista, M., and Frenette, P.S. 2008. Haematopoietic stem cell release is regulated by circadian oscillations. *Nature* 452:442-447.

57. Omatsu, Y., Sugiyama, T., Kohara, H., Kondoh, G., Fujii, N., Kohno, K., and Nagasawa, T. The essential functions of adipo-osteogenic progenitors as the hematopoietic stem and progenitor cell niche. *Immunity* 33:387-399.

58. Sugiyama, T., Kohara, H., Noda, M., and Nagasawa, T. 2006. Maintenance of the hematopoietic stem cell pool by CXCL12-CXCR4 chemokine signaling in bone marrow stromal cell niches. *Immunity* 25:977-988.

59. Warr, M.R., Pietras, E.M., and Passegue, E. Mechanisms controlling hematopoietic stem cell functions during normal hematopoiesis and hematological malignancies. *Wiley Interdiscip Rev Syst Biol Med* 3:681-701.

60. Rando, T.A. 2006. Stem cells, ageing and the quest for immortality. *Nature* 441:1080-1086.

61. Askenasy, N., and Farkas, D.L. 2002. Optical imaging of PKH-labeled hematopoietic cells in recipient bone marrow in vivo. *Stem Cells* 20:501-513.

62. Lo Celso, C., Fleming, H.E., Wu, J.W., Zhao, C.X., Miake-Lye, S., Fujisaki, J., Cote, D., Rowe, D.W., Lin, C.P., and Scadden, D.T. 2009. Live-animal tracking of individual haematopoietic stem/progenitor cells in their niche. *Nature* 457:92-96.

63. Xie, Y., Yin, T., Wiegraebe, W., He, X.C., Miller, D., Stark, D., Perko, K., Alexander, R., Schwartz, J., Grindley, J.C., et al. 2009. Detection of functional haematopoietic stem cell niche using real-time imaging. *Nature* 457:97-101.

64. Lo Celso, C., Wu, J.W., and Lin, C.P. 2009. In vivo imaging of hematopoietic stem cells and their microenvironment. *J Biophotonics* 2:619-631.

65. Flynn, C.M., and Kaufman, D.S. 2007. Donor cell leukemia: insight into cancer stem cells and the stem cell niche. *Blood* 109:2688-2692.

66. Singbrant, S., Askmyr, M., Purton, L.E., and Walkley, C.R. Defining the hematopoietic stem cell niche: the chicken and the egg conundrum. *J Cell Biochem* 112:1486-1490.

67. Li, L., and Clevers, H. Coexistence of quiescent and active adult stem cells in mammals. *Science* 327:542-545.

68. Wilson, A., Laurenti, E., Oser, G., van der Wath, R.C., Blanco-Bose, W., Jaworski, M., Offner, S., Dunant, C.F., Eshkind, L., Bockamp, E., et al. 2008. Hematopoietic stem cells reversibly switch from dormancy to self-renewal during homeostasis and repair. *Cell* 135:1118-1129.

69. Davies, E.L., and Fuller, M.T. 2008. Regulation of self-renewal and differentiation in adult stem cell lineages: lessons from the Drosophila male germ line. *Cold Spring Harb Symp Quant Biol* 73:137-145.

70. DeGowin, R.L., Gibson, D.P., Knapp, S.A., and Wathen, L.M. 1981. Tumor-induced suppression of marrow stromal colonies. *Exp Hematol* 9:811-819.

71. Wathen, L.M., Knapp, S.A., and DeGowin, R.L. 1981. Suppression of marrow stromal cells and microenvironmental damage following sequential radiation and cyclophosphamide. *Int J Radiat Oncol Biol Phys* 7:935-941.

72. Haylock, D.N., Williams, B., Johnston, H.M., Liu, M.C., Rutherford, K.E., Whitty, G.A., Simmons, P.J., Bertoncello, I., and Nilsson, S.K. 2007. Hemopoietic stem cells with higher hemopoietic potential reside at the bone marrow endosteum. *Stem Cells* 25:1062-1069.

73. Kiel, M.J., Acar, M., Radice, G.L., and Morrison, S.J. 2009. Hematopoietic stem cells do not depend on N-cadherin to regulate their maintenance. *Cell Stem Cell* 4:170-179.

74. Kiel, M.J., Radice, G.L., and Morrison, S.J. 2007. Lack of evidence that hematopoietic stem cells depend on N-cadherin-mediated adhesion to osteoblasts for their maintenance. *Cell Stem Cell* 1:204-217.

75. Weksberg, D.C., Chambers, S.M., Boles, N.C., and Goodell, M.A. 2008. CD150- side population cells represent a functionally distinct population of long-term hematopoietic stem cells. *Blood* 111:2444-2451.

76. Kiel, M.J., and Morrison, S.J. 2006. Maintaining hematopoietic stem cells in the vascular niche. *Immunity* 25:862-864

.

77. Kiel, M.J., Yilmaz, O.H., and Morrison, S.J. 2008. CD150- cells are transiently reconstituting multipotent progenitors with little or no stem cell activity. *Blood* 111:4413-4414; author reply 4414-4415.

78. Ogawa, M., Tajima, F., Ito, T., Sato, T., Laver, J.H., and Deguchi, T. 2001. CD34 expression by murine hematopoietic stem cells. Developmental changes and kinetic alterations. *Ann N Y Acad Sci* 938:139-145.

79. Yang, L., Bryder, D., Adolfsson, J., Nygren, J., Mansson, R., Sigvardsson, M., and Jacobsen, S.E. 2005. Identification of Lin(-)Sca1(+)kit(+)CD34(+)Flt3- short-term hematopoietic stem cells capable of rapidly reconstituting and rescuing myeloablated transplant recipients. *Blood* 105:2717-2723.

80. Jacobson, L.O., Marks, E.K., and et al. 1949. The role of the spleen in radiation injury. *Proc Soc Exp Biol Med* 70:740-742.

81. Barnes, D.W., Corp, M.J., Loutit, J.F., and Neal, F.E. 1956. Treatment of murine leukaemia with X rays and homologous bone marrow; preliminary communication. *Br Med J* 2:626-627.

82. Lorenz, E., Uphoff, D., Reid, T.R., and Shelton, E. 1951. Modification of irradiation injury in mice and guinea pigs by bone marrow injections. *J Natl Cancer Inst* 12:197-201.

83. Thomas, E.D. 1995. History, current results, and research in marrow transplantation. *Perspect Biol Med* 38:230-237.

BIOGRAPHICAL SKETCH

Seungbum Kim was born in January of 1977, in Seoul, Korea. After receiving his Bachelor and Master of Science degrees in life science from Korea University, Seungbum enrolled into the Interdisciplinary Program in Biomedical Sciences at the University of Florida in August of 2006. He joined the laboratory of Dr. Edward Scott and studied in vivo imaging techniques of hematopoietic stem cell engraftment in mouse. He received his Ph.D. in December 2011. As his scientific achievements, he has a first author paper in Laboratory Investigation and he is the co-authors in several scientific journals such as Leukemia, Transplantation and Biochemical and Biophysical Research Communications. He also has two additional first author articles currently under submission. He presented his works in international meetings such as the 2010 International Society for Stem Cell Research meeting and 2011 American Society for Hematology meeting.